TICRA

In-flight Retrieval of Geometrical information on the Planck Telescope

RFM2

RF performance of LFI beams

Author: Per Heighwood Nielsen

December, 2015 S-1563-14

TICRA
LÆDERSTRÆDE 34 · DK-1201 COPENHAGEN K DENMARK
TELEPHONE +45 33 12 45 72 TELEFAX +45 33 12 08 80
E-MAIL ticra@ticra.com http://www.ticra.com

VAT REGISTRATION NO. DK-1055 8697
TICRA FOND, CVR REG. NO. 1055 8697

TABLE OF CONTENTS

1. Introduction.

The present study is prepared for ESTEC under contract no. 18395/04/NL/NB, CCN no. 8.

The title of the work is

"In-flight Retrieval of Geometrical information on the Planck Telescope"

This Report presents a computation of all the LFI beam patterns using the retrieved telescope geometry RFM2 developed in Report S-1563-13. The RFM2 geometry is replicated in Appendix A. The patterns are compared with the fitted deconvoluted measured patterns from Report S-1563-09 to visualize the remaining differences.

All calculated patterns are analysed at the centre frequency using Physical Optics on both mirrors and calculated in uv directions defined in the Field-of-View, FOV, coordinate system as

$$u = \sin(\theta)\cos(\varphi)$$
$$v = \sin(\theta)\sin(\varphi)$$

The radiation from the planets is unpolarized so both co- and cross-components of the calculated radiated field are measured. Therefore, all field data from the planet scan is given as power only.

2. RF performance of LFI beams.

The final RF performance of the retrieved telescope geometry model, RFM2, and for all LFI detector positions are given in the following Figure 2-1 to Figure 2-22. The calculated performances are compared with the fitted deconvoluted measured beams down to their respective noise levels in contour plots, where the full lines are for the measured field.

Both the measured and the retrieved main beams are azimuthally integrated in steps down to the noise level for the individual beams. The total power from the measured beam is equalized to the power of the calculated retrieved beam. The angular power distributions are then compared and shown together with the differences between these two integrated powers. The equalization gives a normalization of the measured beam and the zero shown near the end of the difference plot.

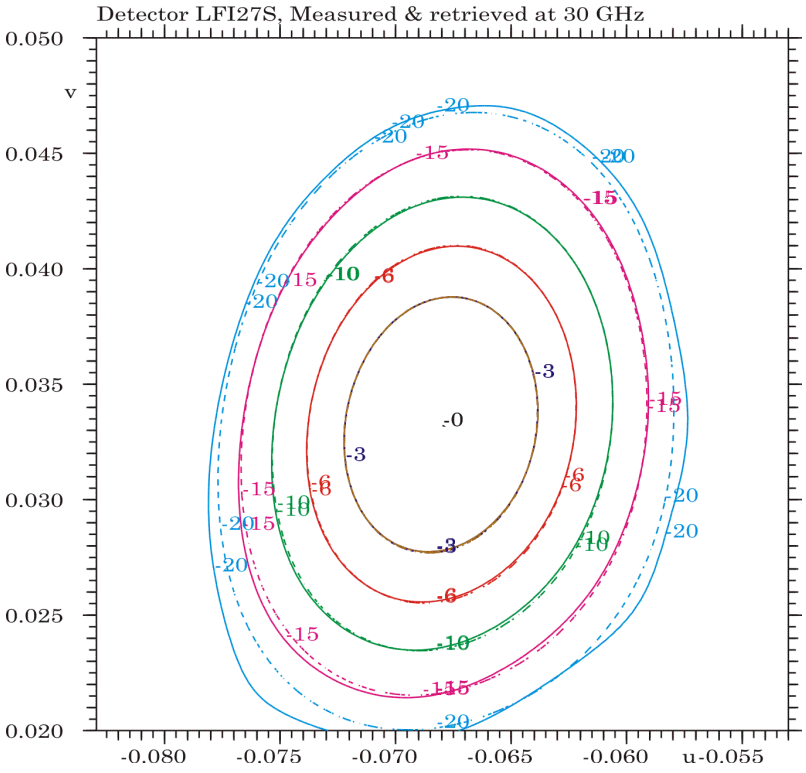

a) Measured (full line) and retrieved (dashed) power pattern

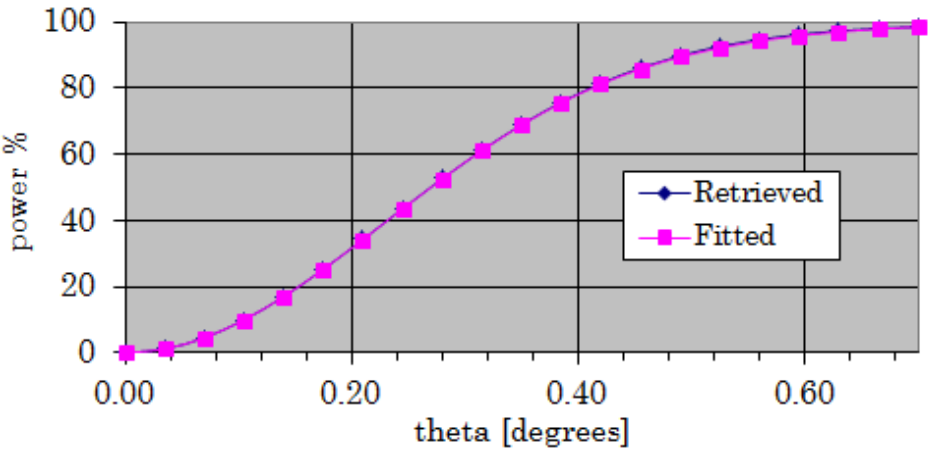

b) Azimuthally integrated power

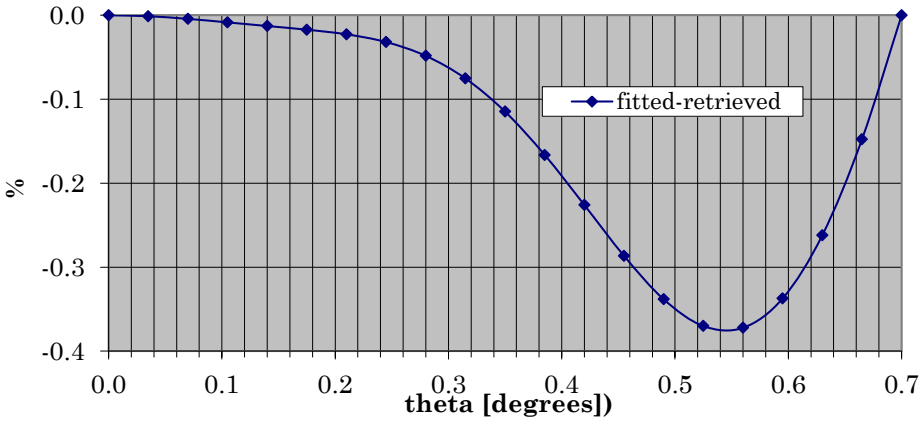

c) Difference

Figure 2-1 Kriging fitted measured and retrieved power pattern for 30 GHz detector, LFI27S.

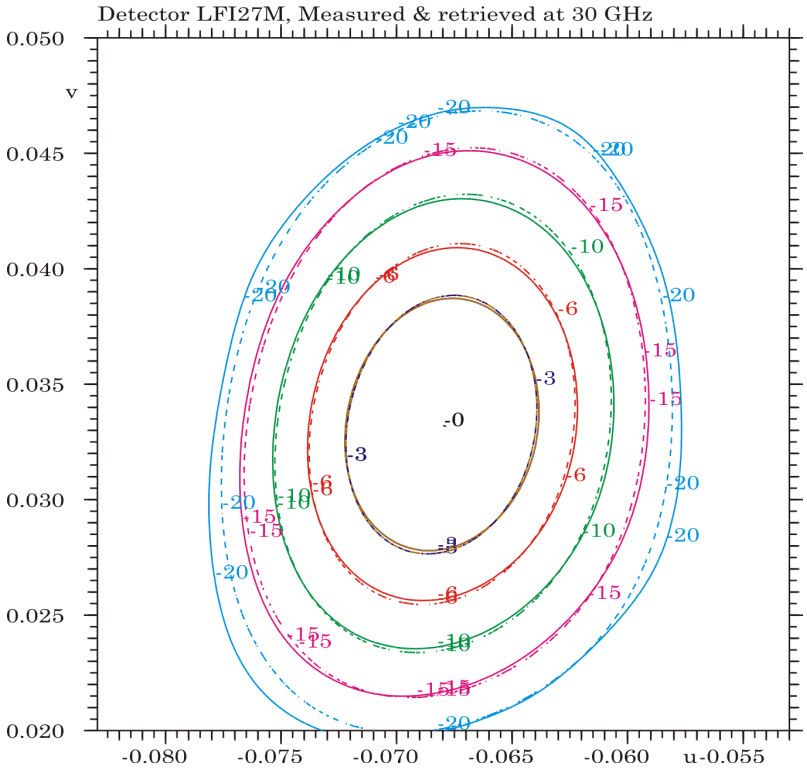

a) Measured (full line) and retrieved (dashed) power pattern

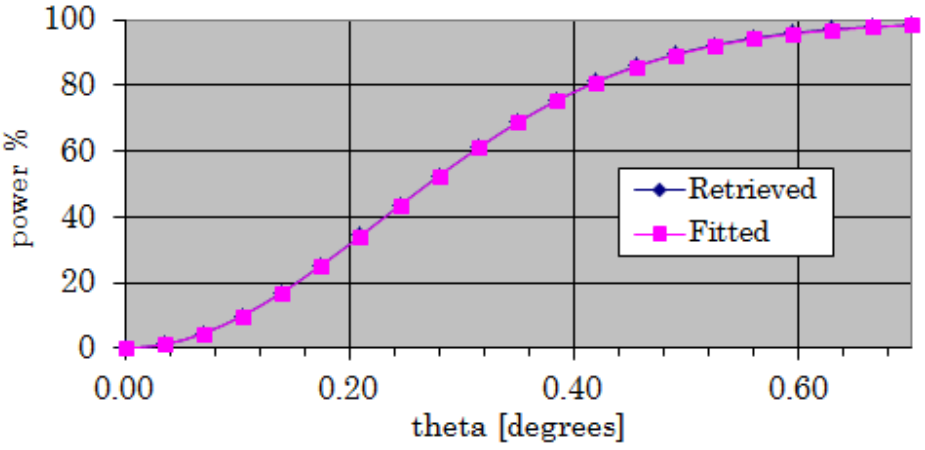

b) Azimuthally integrated power

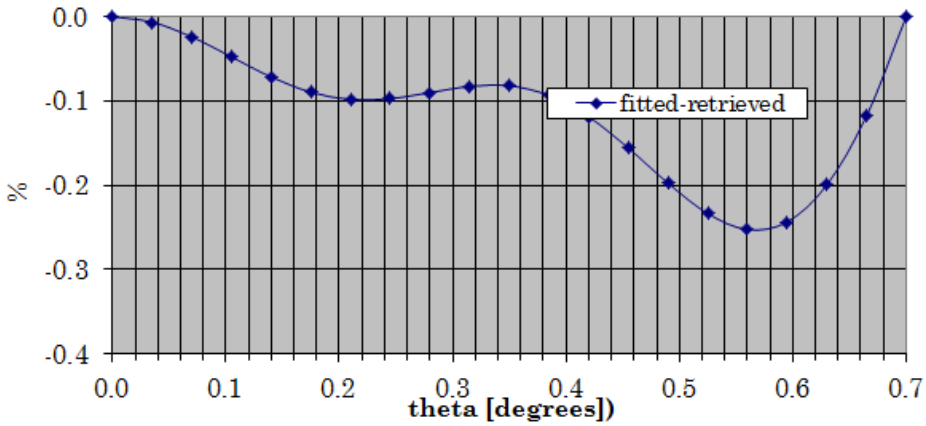

c) Difference

Figure 2-2 Kriging fitted measured and retrieved power pattern for 30 GHz detector, LFI27M.

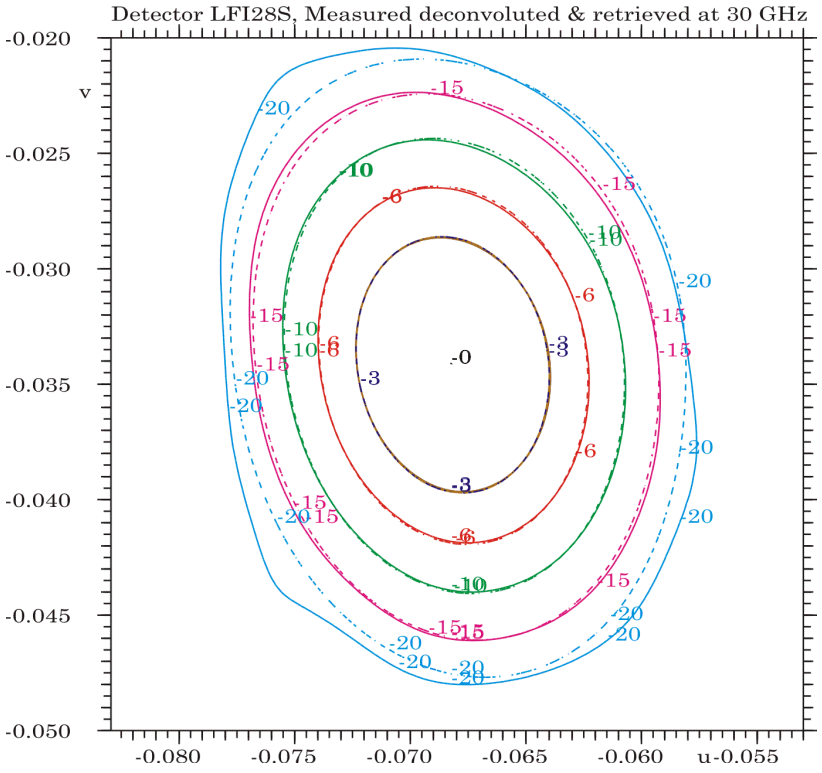

a) Measured (full line) and retrieved (dashed) power pattern

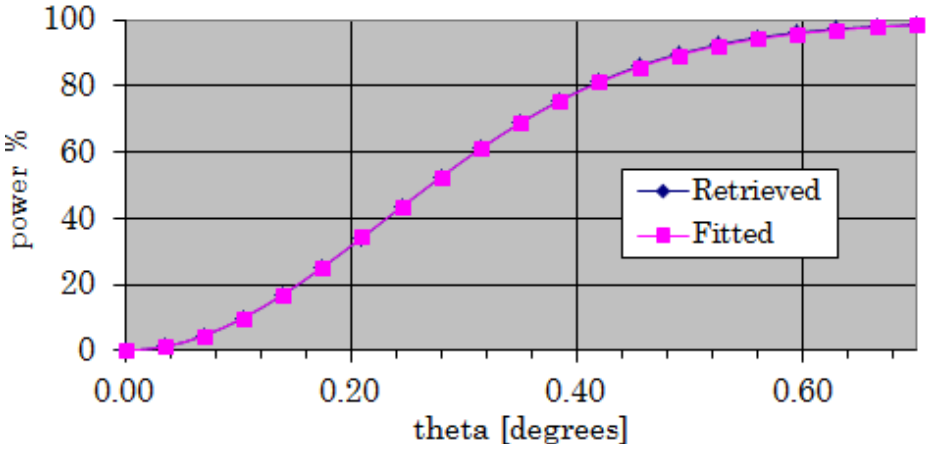

b) Azimuthally integrated power

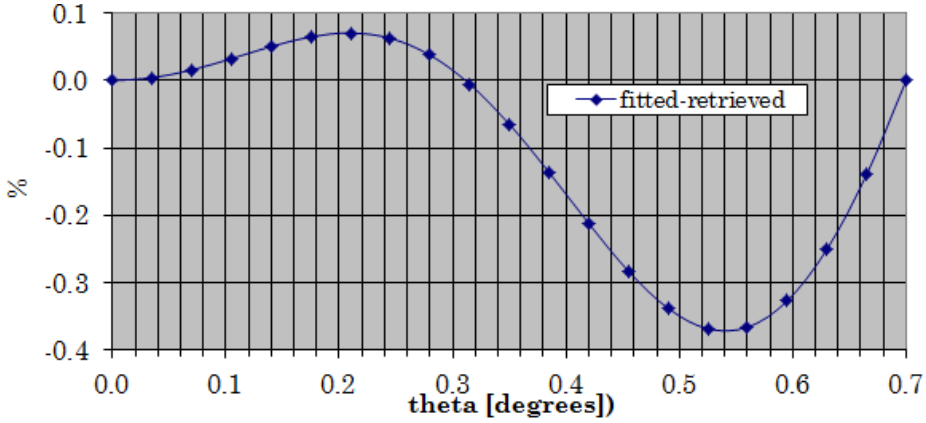

c) Difference

Figure 2-3 Kriging fitted measured and retrieved power pattern for 30 GHz detector, LFI28S.

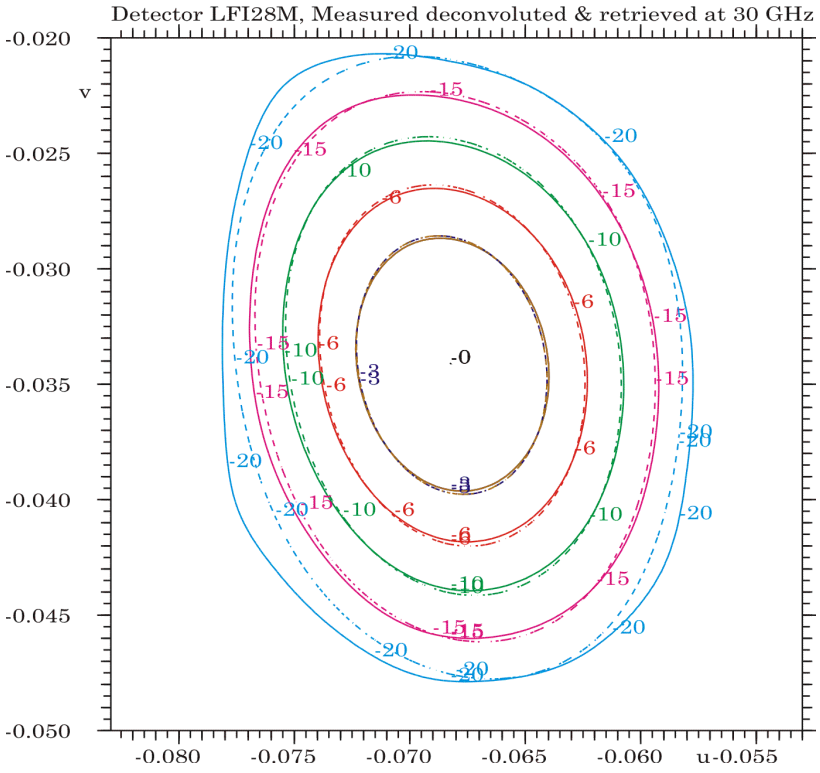

a) Measured (full line) and retrieved (dashed) power pattern

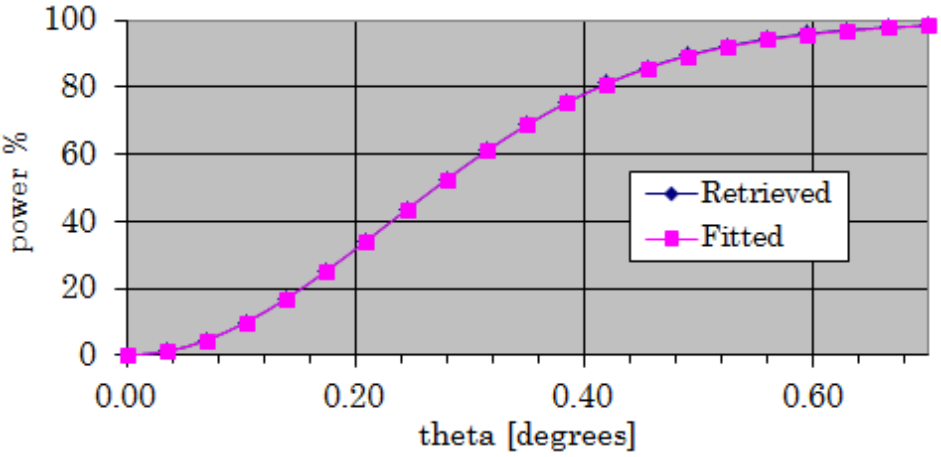

b) Azimuthally integrated power

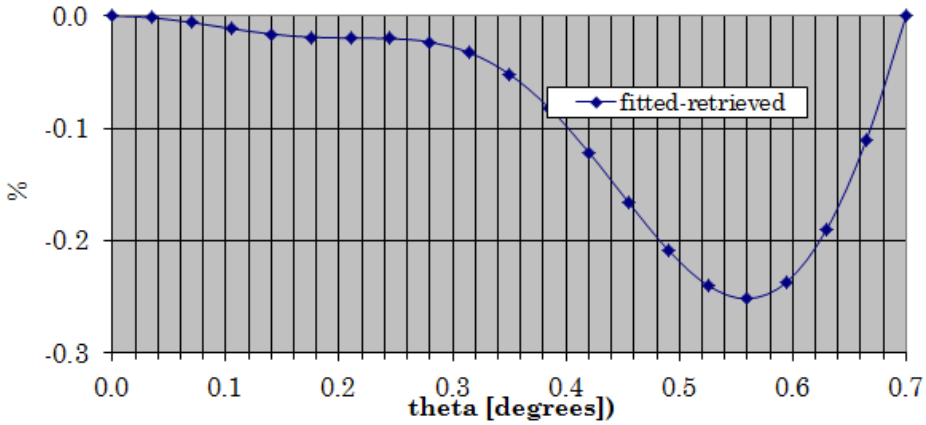

c) Difference

Figure 2-4 Kriging fitted measured and retrieved power pattern for 30 GHz detector, LFI28M.

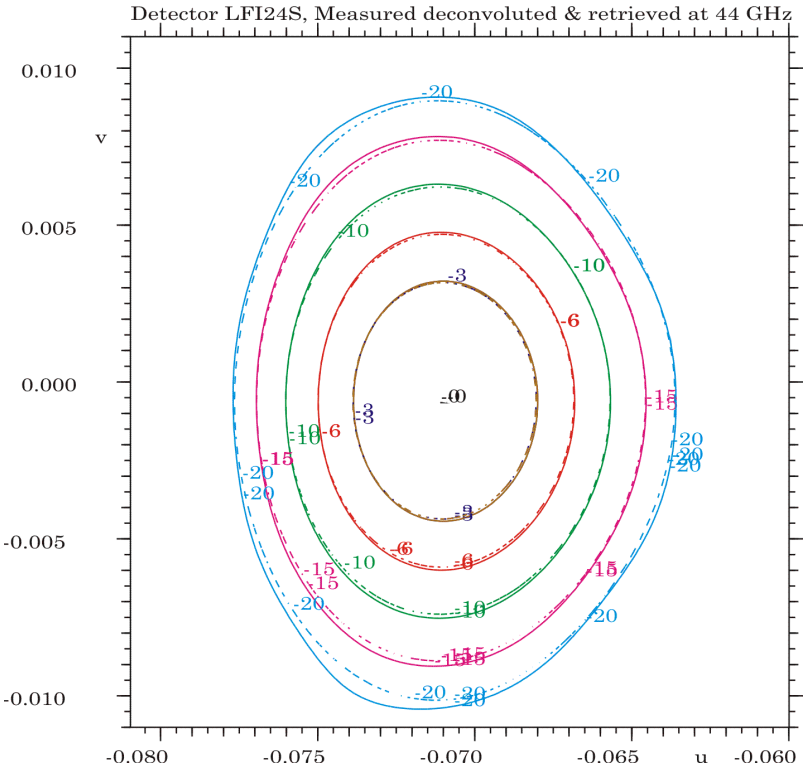

a) Measured (full line) and retrieved (dashed) power pattern

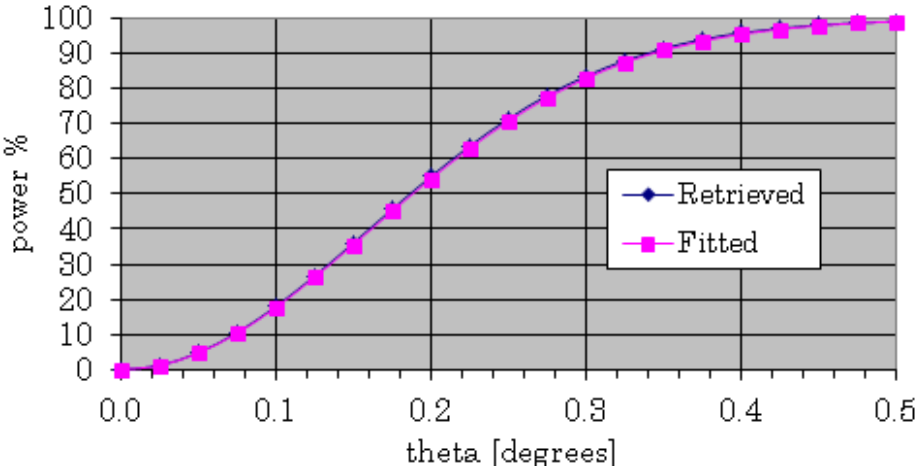

b) Azimuthally integrated power

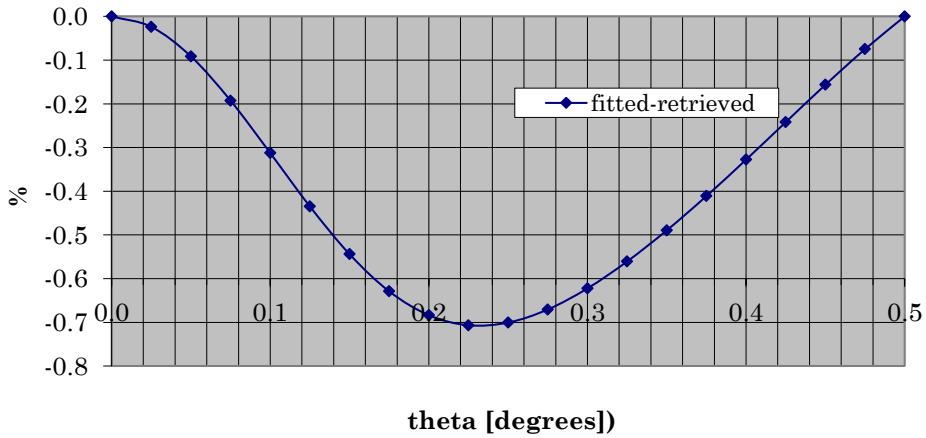

c) Difference

Figure 2-5 Kriging fitted measured and retrieved power pattern for 44 GHz detector, LFI24S.

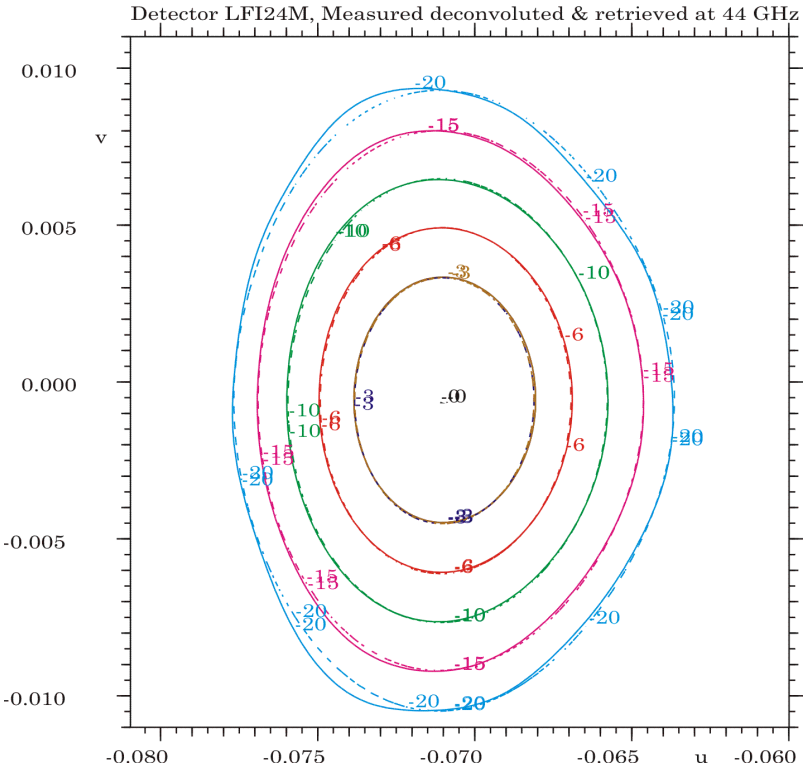

a) Measured (full line) and retrieved (dashed) power pattern

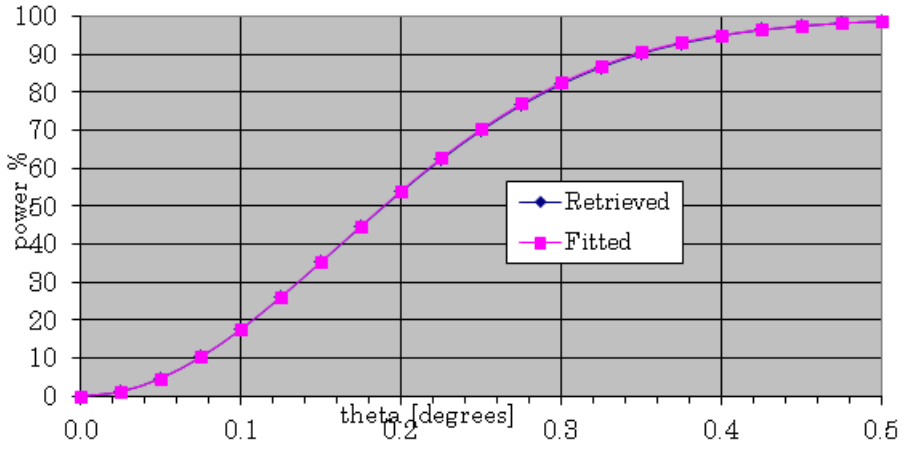

b) Azimuthally integrated power

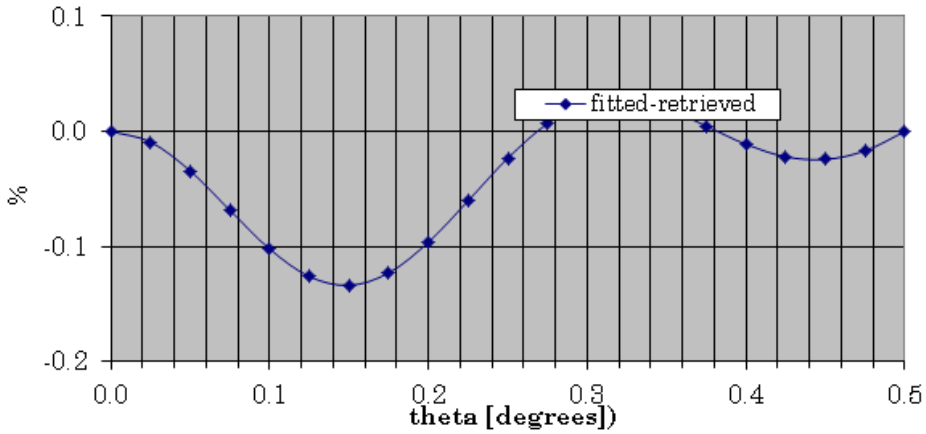

c) Difference

Figure 2-6 Kriging fitted measured and retrieved power pattern for 44 GHz detector, LFI24M.

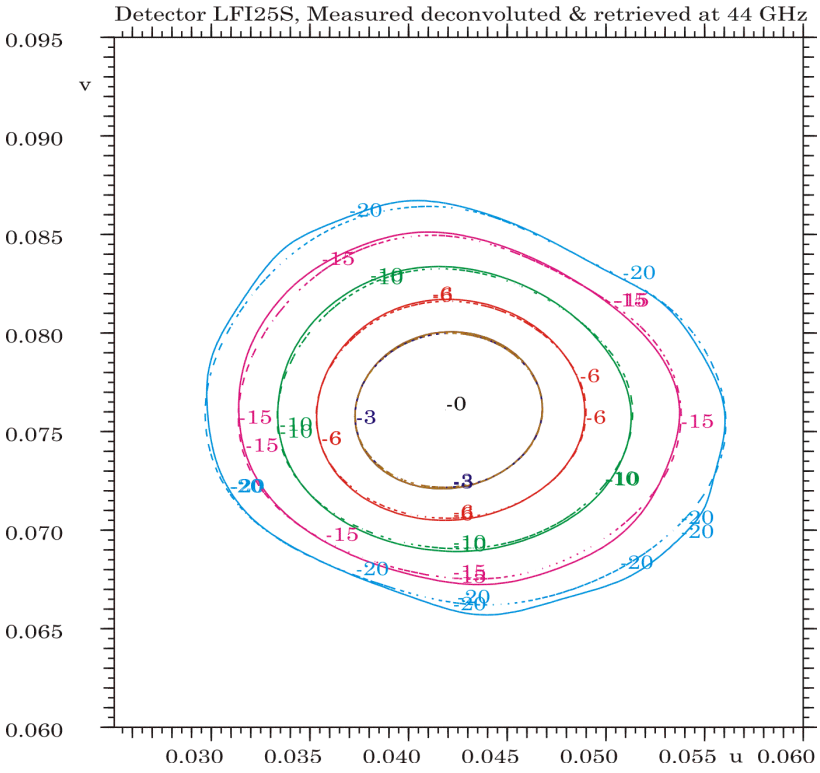

a) Measured (full line) and retrieved (dashed) power pattern

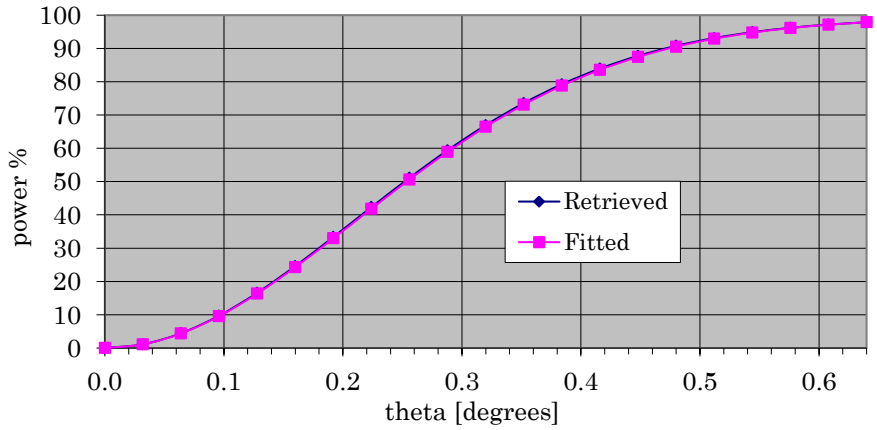

b) Azimuthally integrated power

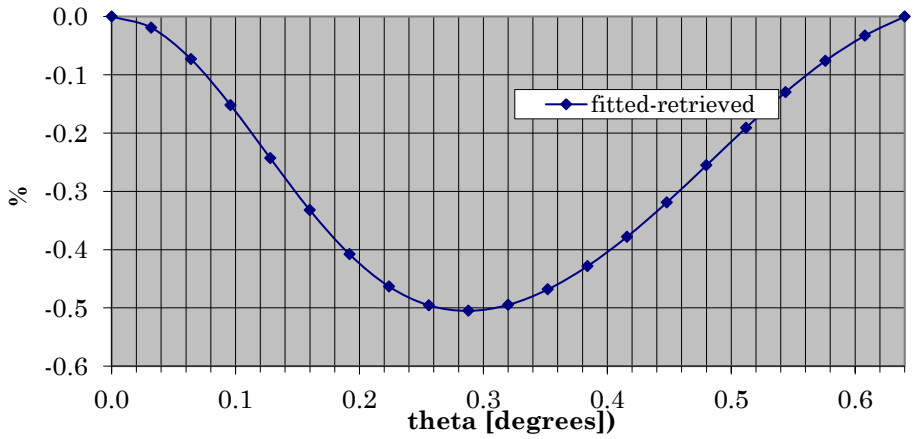

c) Difference

Figure 2-7 Kriging fitted measured and retrieved power pattern for 44 GHz detector, LFI25S.

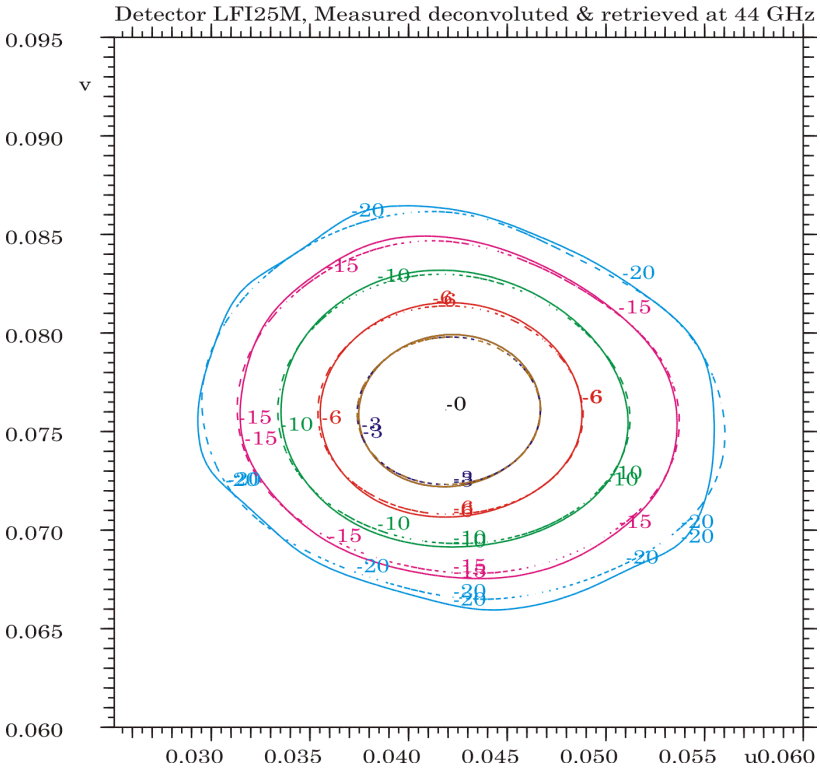

a) Measured (full line) and retrieved (dashed) power pattern

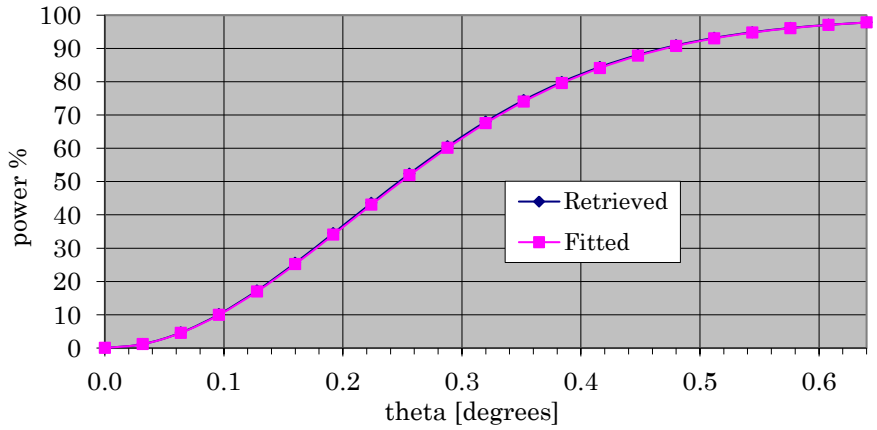

b) Azimuthally integrated power

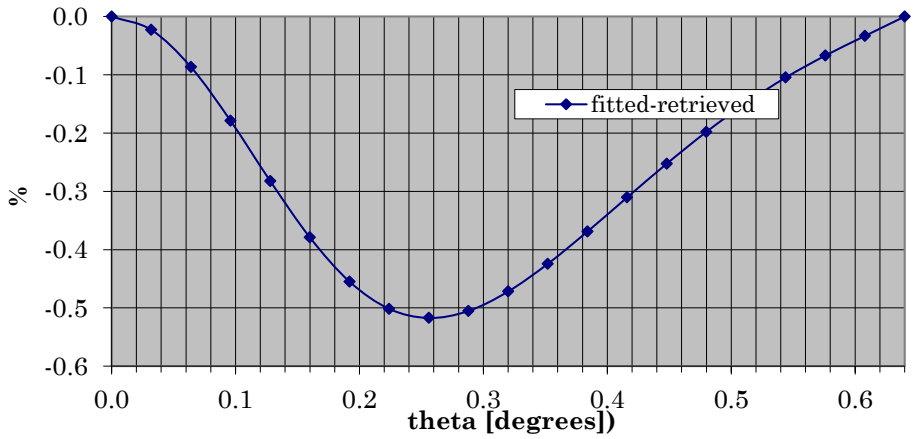

c) Difference

Figure 2-8 Kriging fitted measured and retrieved power pattern for 44 GHz detector, LFI25M.

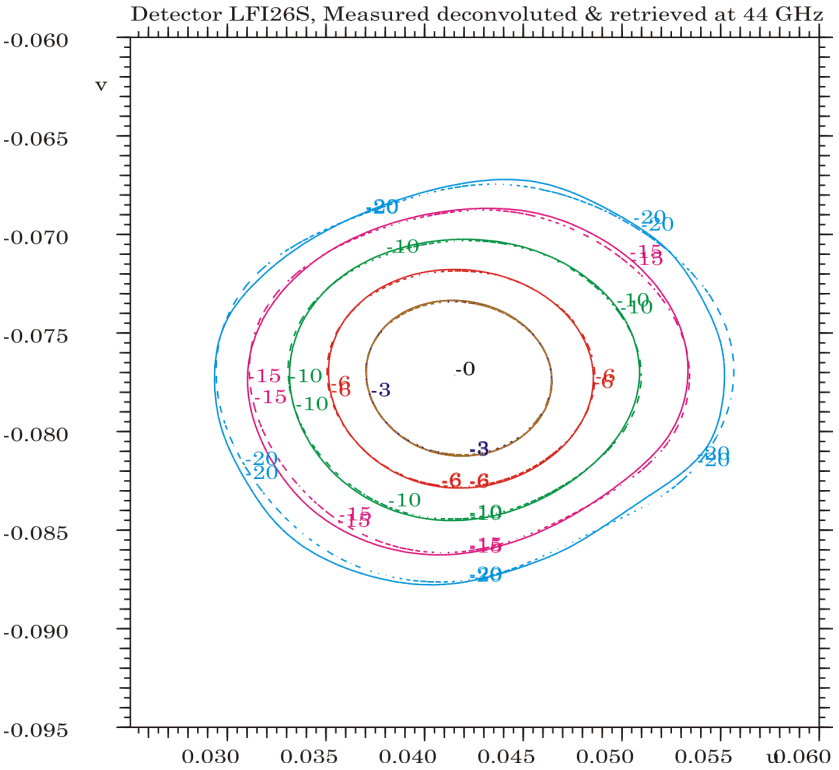

a) Measured (full line) and retrieved (dashed) power pattern

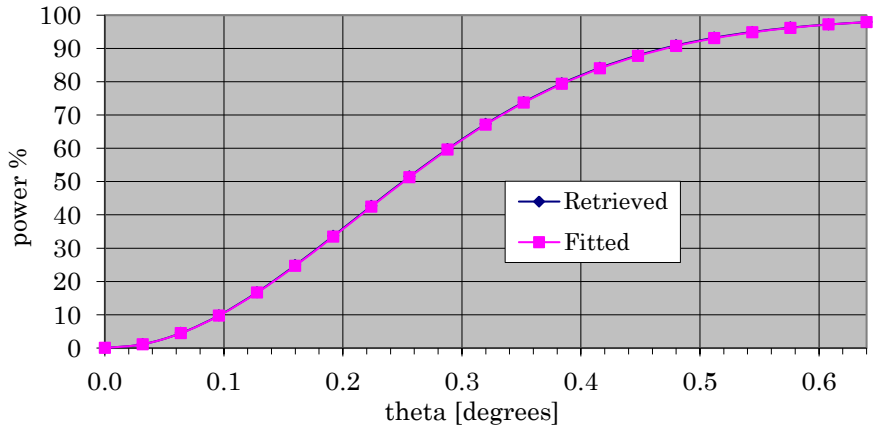

b) Azimuthally integrated power

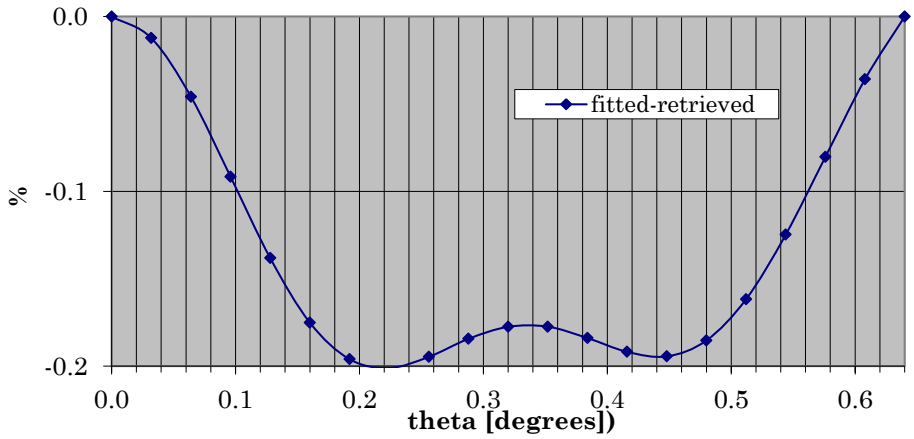

c) Difference

Figure 2-9 Kriging fitted measured and retrieved power pattern for 44 GHz detector, LFI26S.

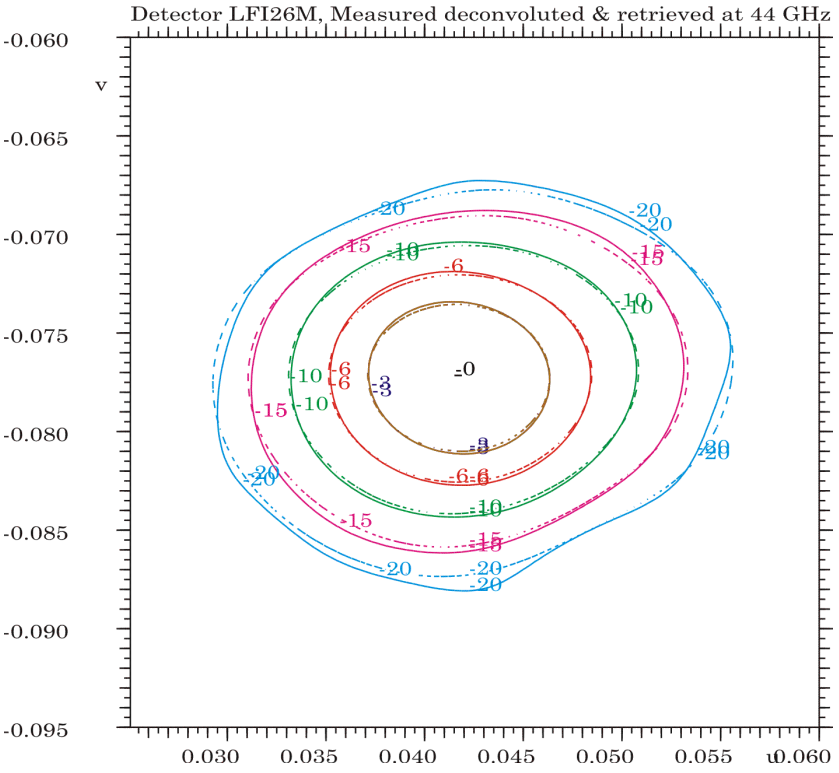

a) Measured (full line) and retrieved (dashed) power pattern

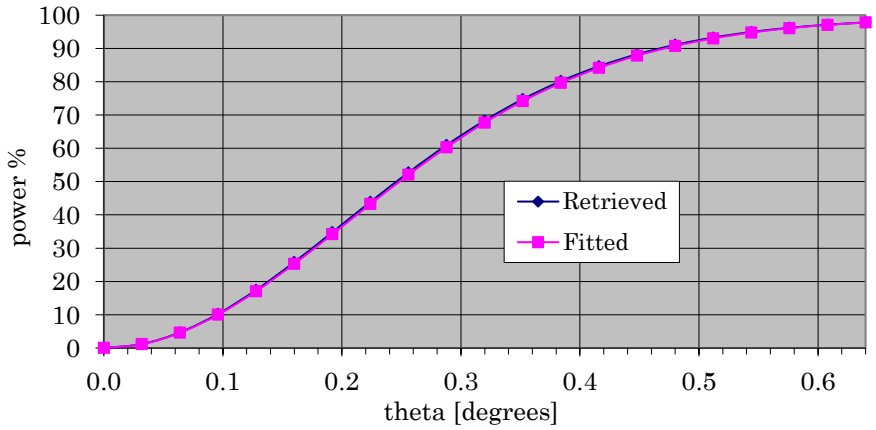

b) Azimuthally integrated power

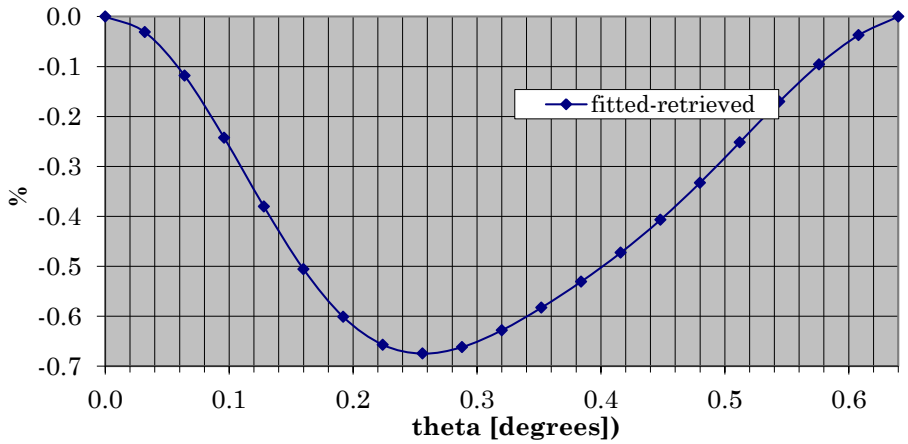

c) Difference

Figure 2-10 Kriging fitted measured and retrieved power pattern for 44 GHz detector, LFI26M.

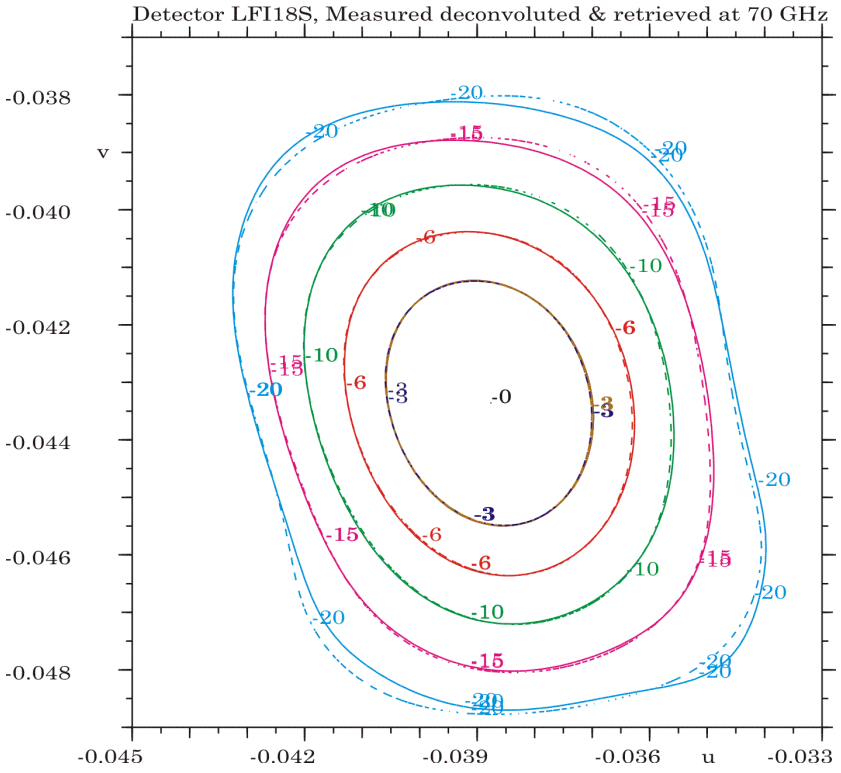

a) Measured (full line) and retrieved (dashed) power pattern

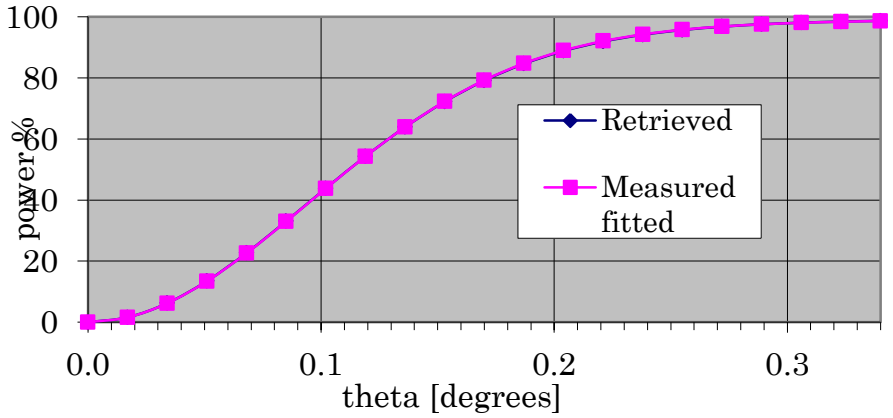

b) Azimuthally integrated power

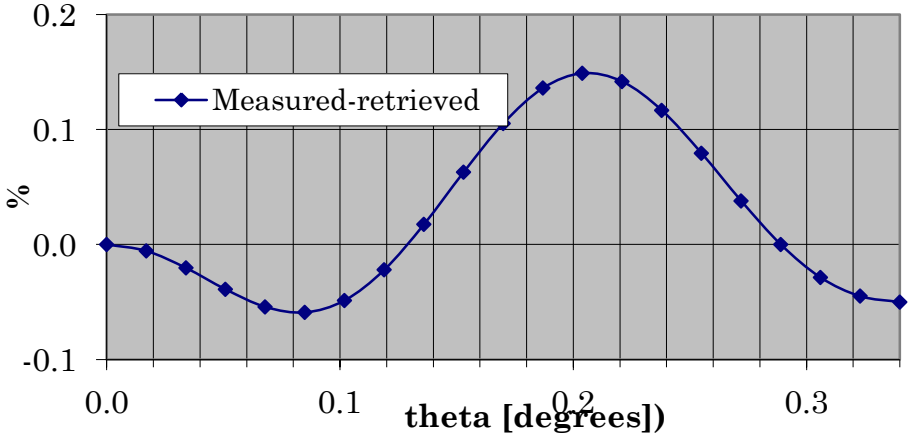

c) Difference

Figure 2-11 Kriging fitted measured and retrieved power pattern for 70 GHz detector, LFI18S.

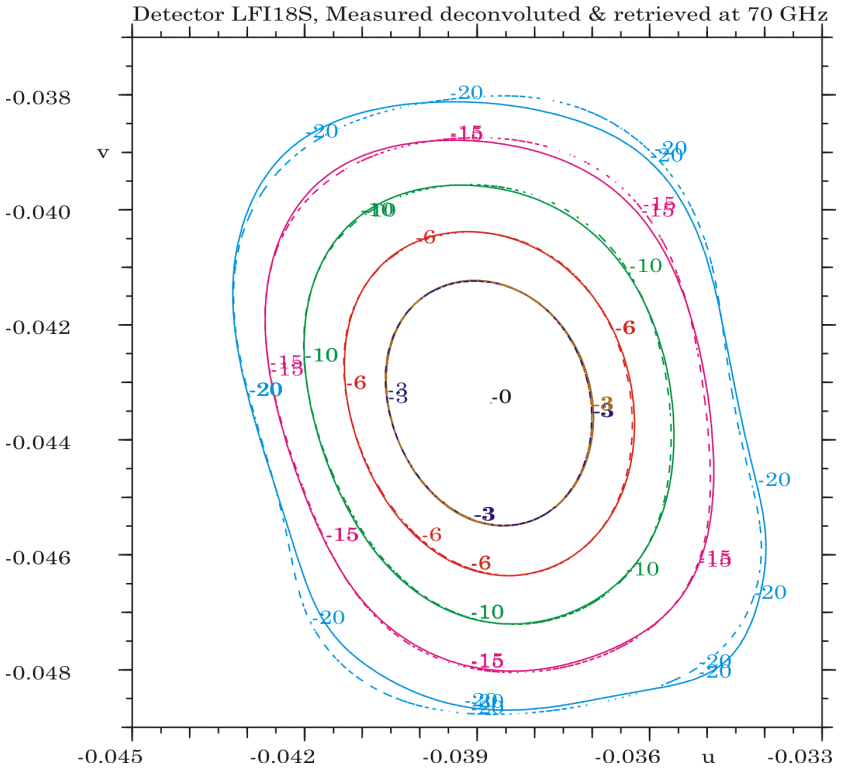

a) Measured (full line) and retrieved (dashed) power pattern

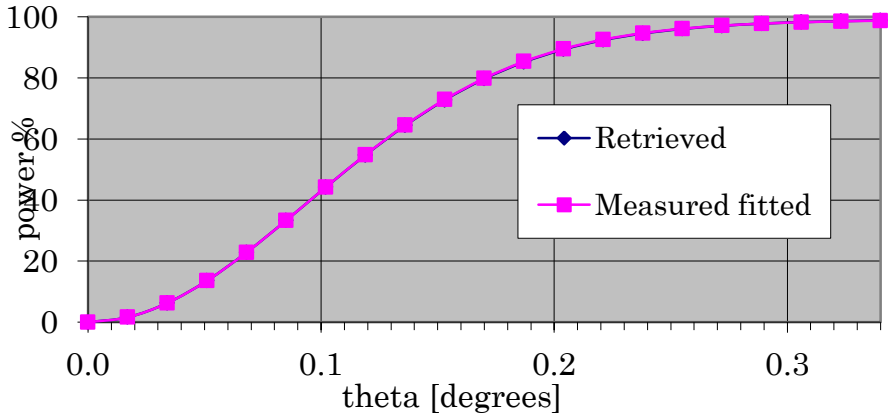

b) Azimuthally integrated power

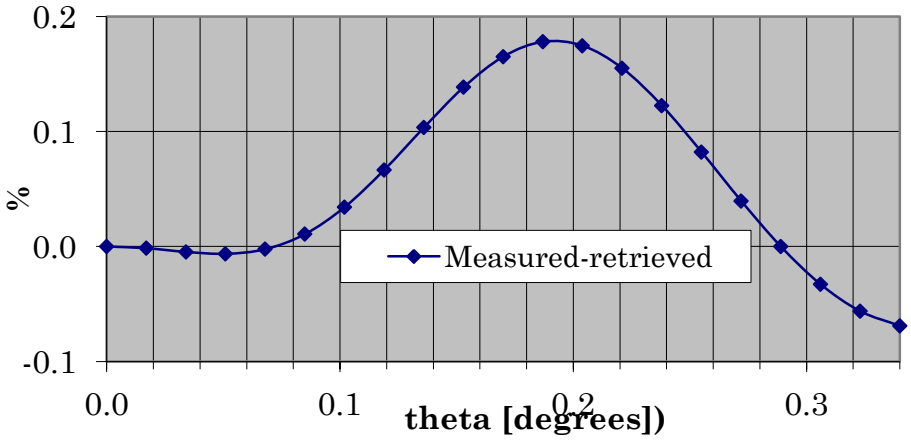

c) Difference

Figure 2-12 Kriging fitted measured and retrieved power pattern for 70 GHz detector, LFI18M.

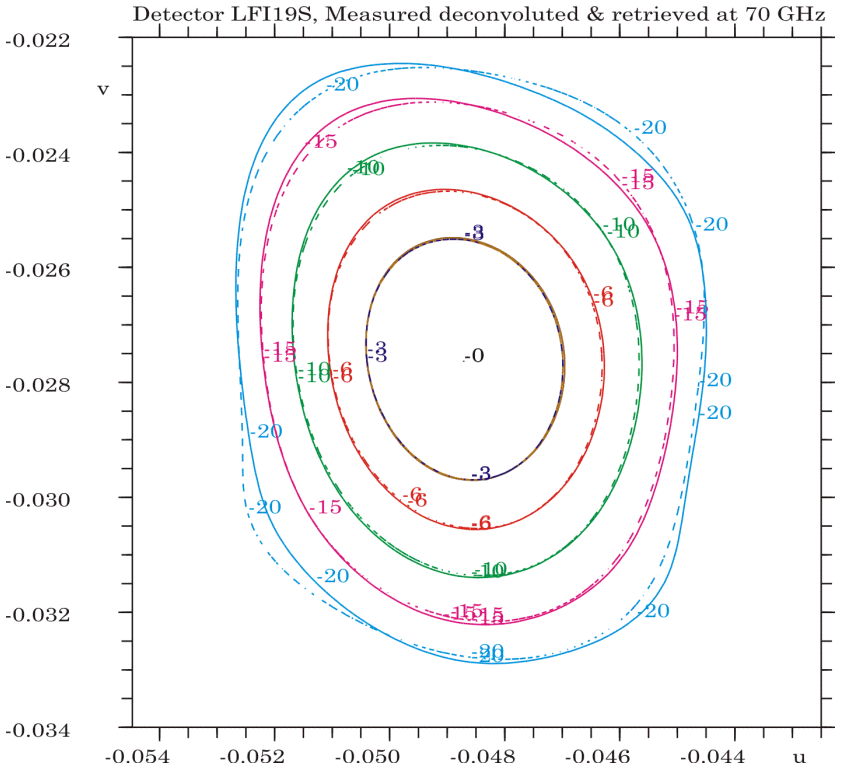

a) Measured (full line) and retrieved (dashed) power pattern

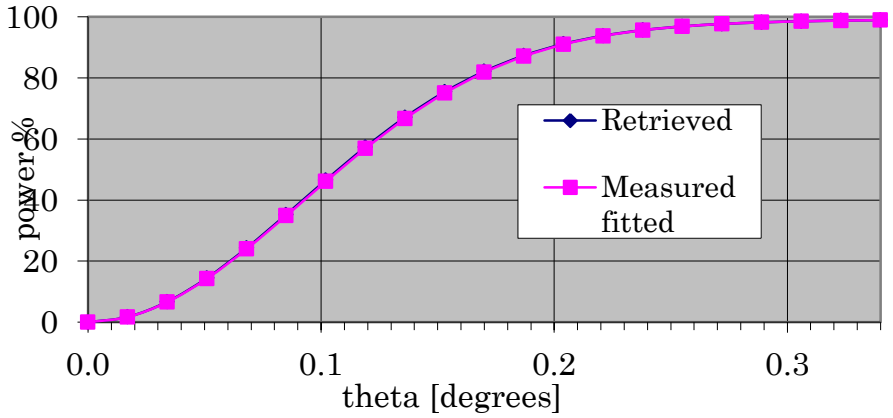

b) Azimuthally integrated power

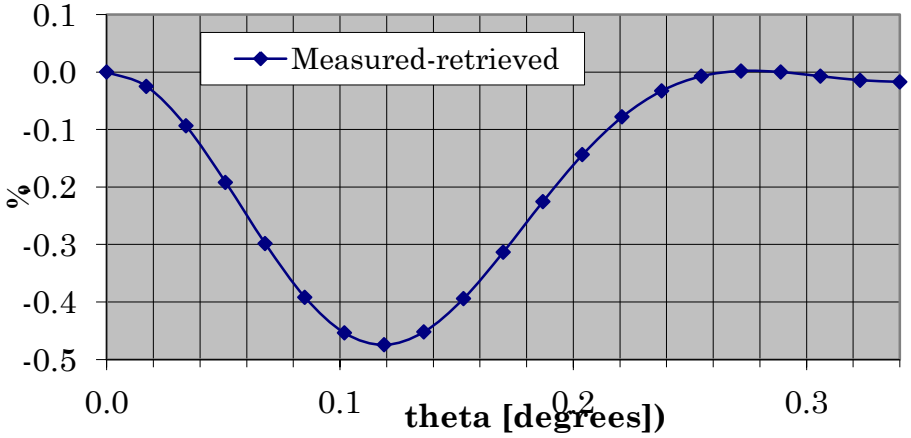

c) Difference

Figure 2-13 Kriging fitted measured and retrieved power pattern for 70 GHz detector, LFI19S.

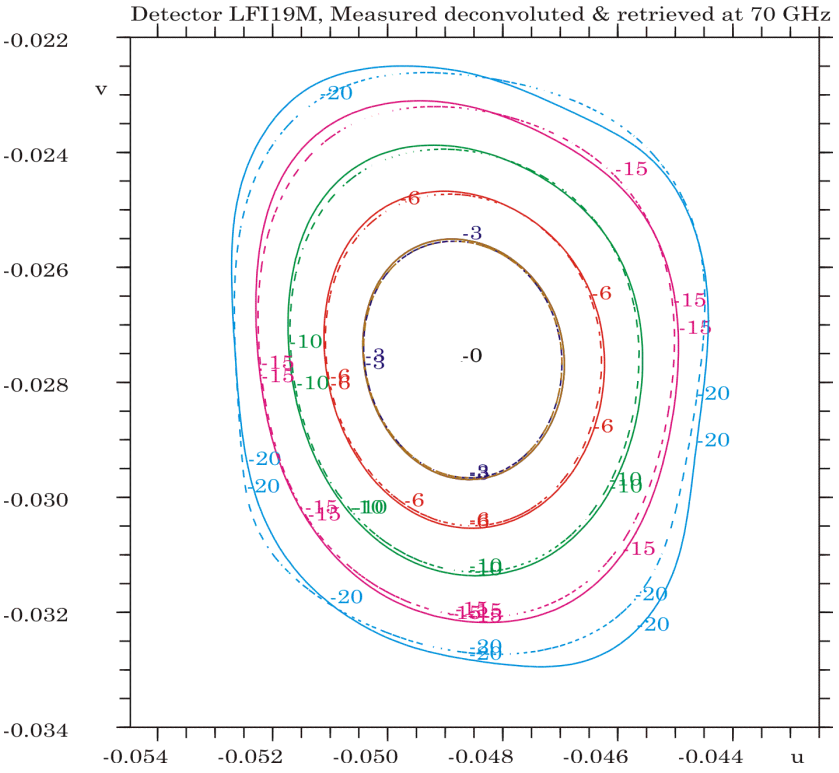

a) Measured (full line) and retrieved (dashed) power pattern

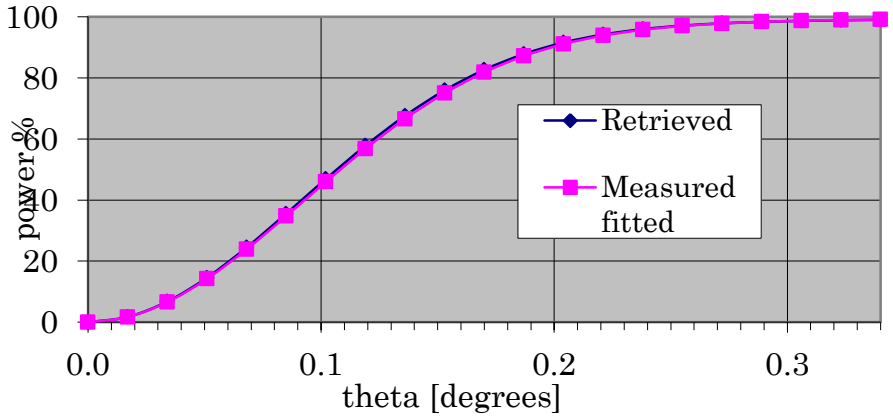

b) Azimuthally integrated power

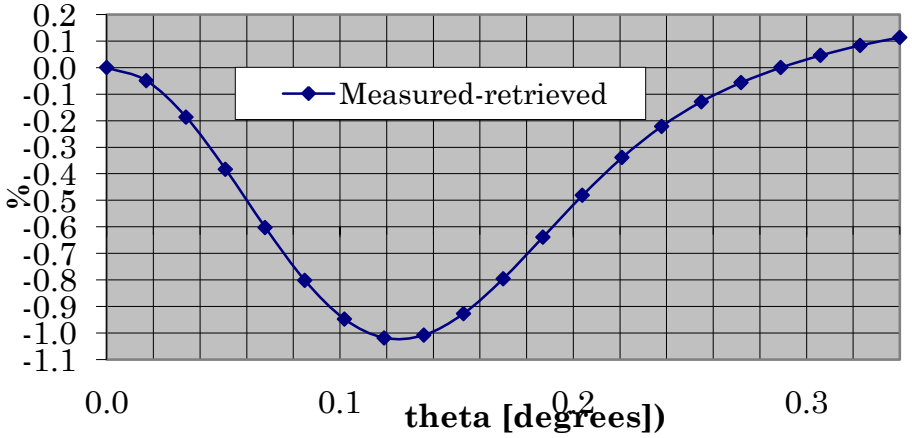

c) Difference

Figure 2-14 Kriging fitted measured and retrieved power pattern for 70 GHz detector, LFI19M.

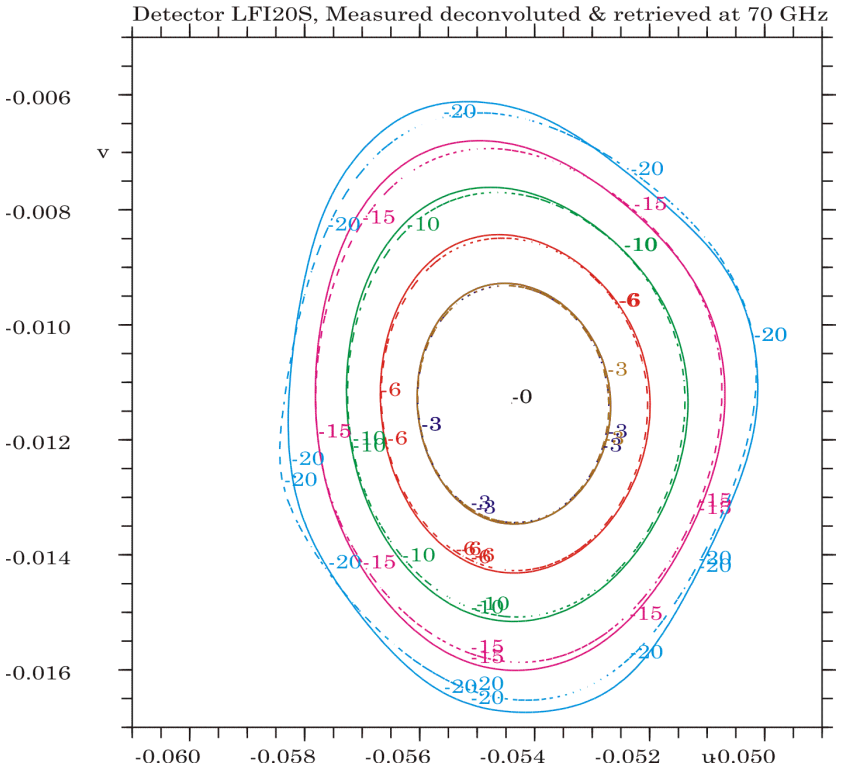

a) Measured (full line) and retrieved (dashed) power pattern

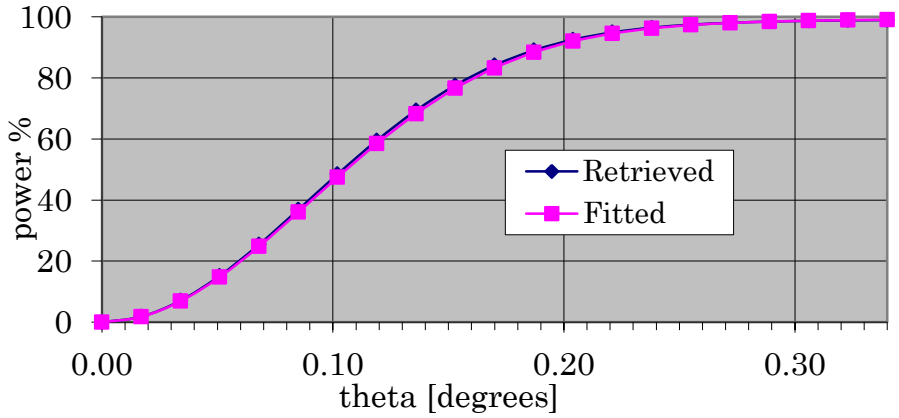

b) Azimuthally integrated power

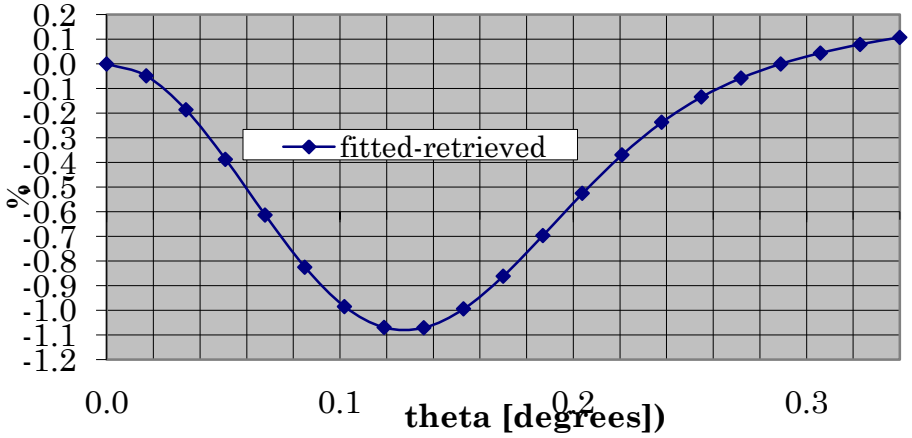

c) Difference

Figure 2-15 Kriging fitted measured and retrieved power pattern for 70 GHz detector, LFI20S.

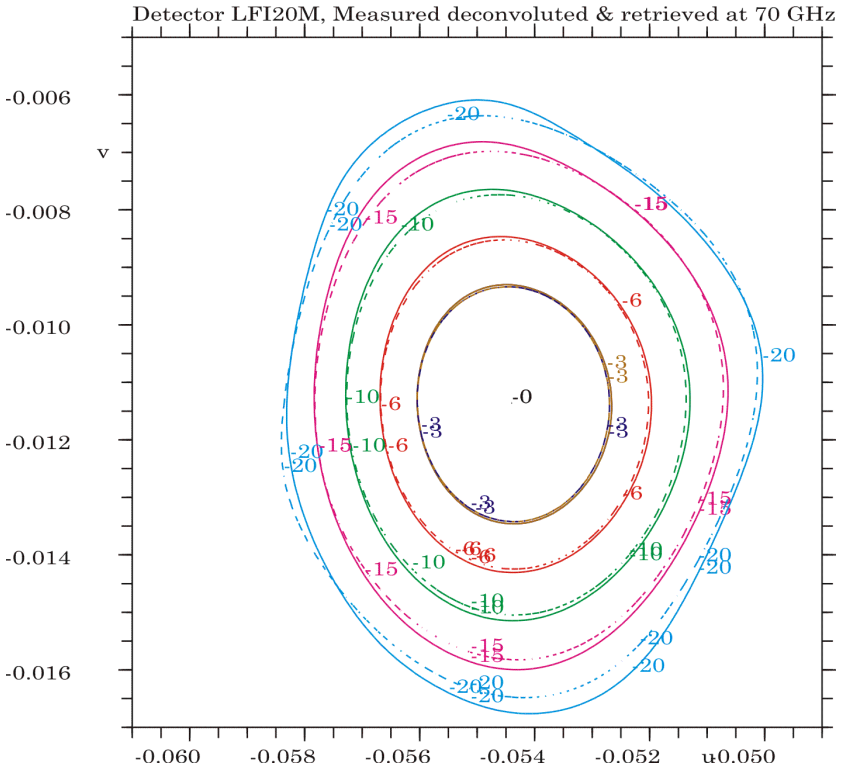

a) Measured (full line) and retrieved (dashed) power pattern

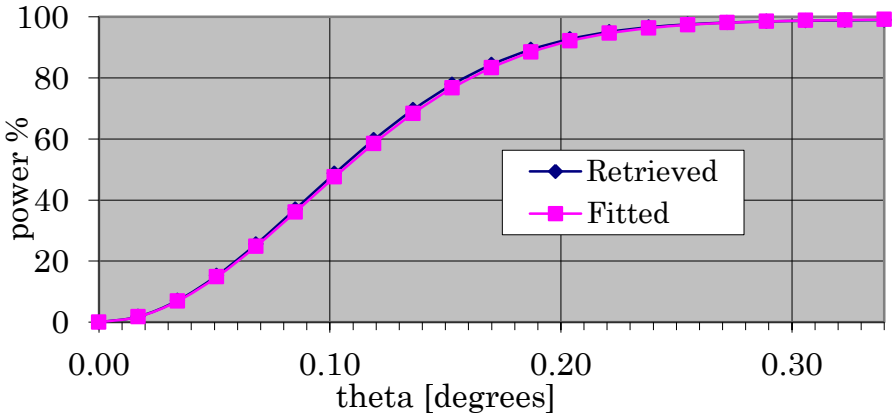

b) Azimuthally integrated power

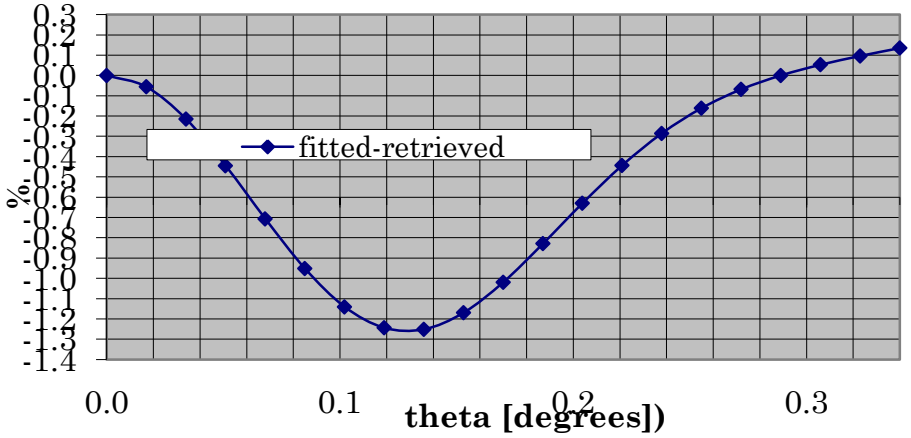

c) Difference

Figure 2-16 Kriging fitted measured and retrieved power pattern for 70 GHz detector, LFI20M.

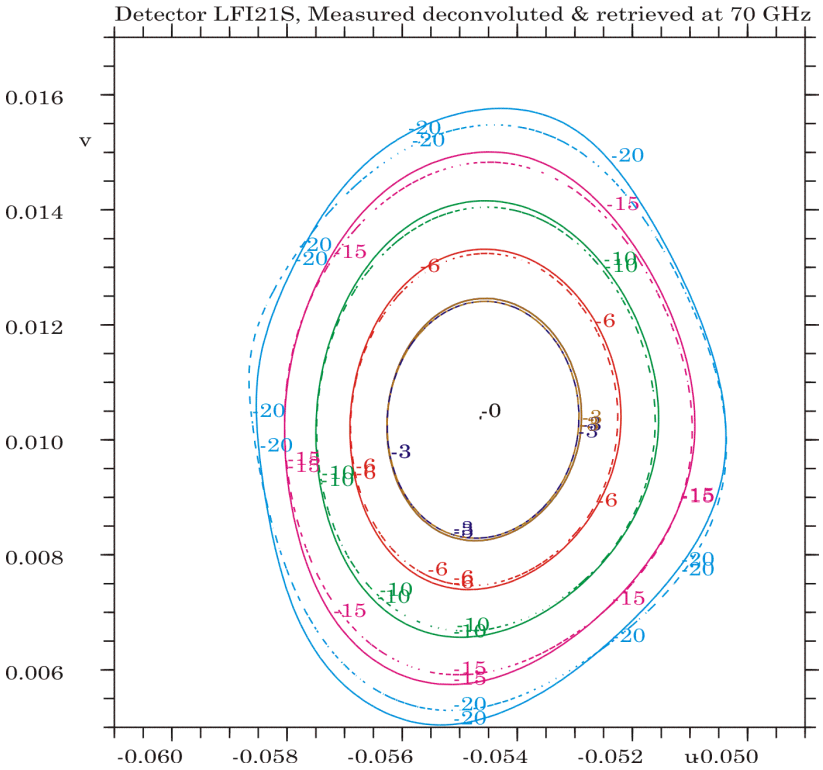

a) Measured (full line) and retrieved (dashed) power pattern

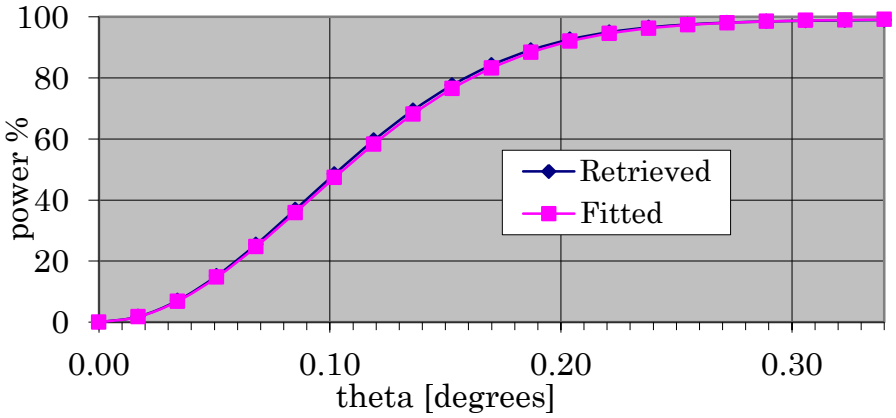

b) Azimuthally integrated power

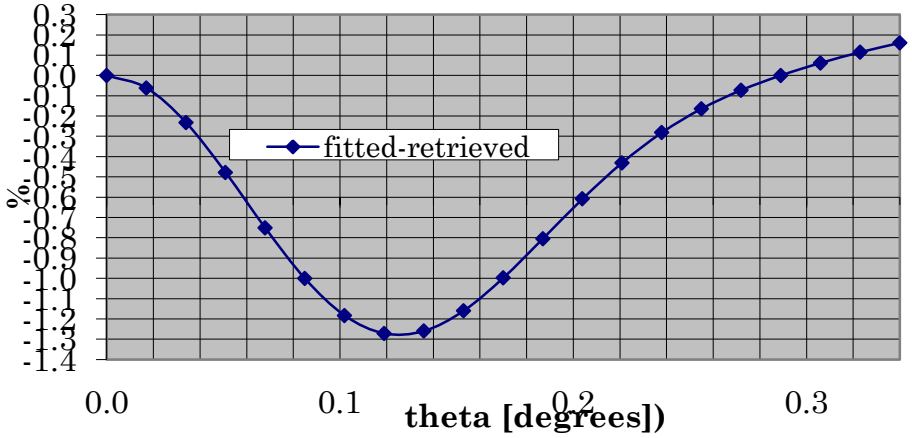

c) Difference

Figure 2-17 Kriging fitted measured and retrieved power pattern for 70 GHz detector, LFI21S.

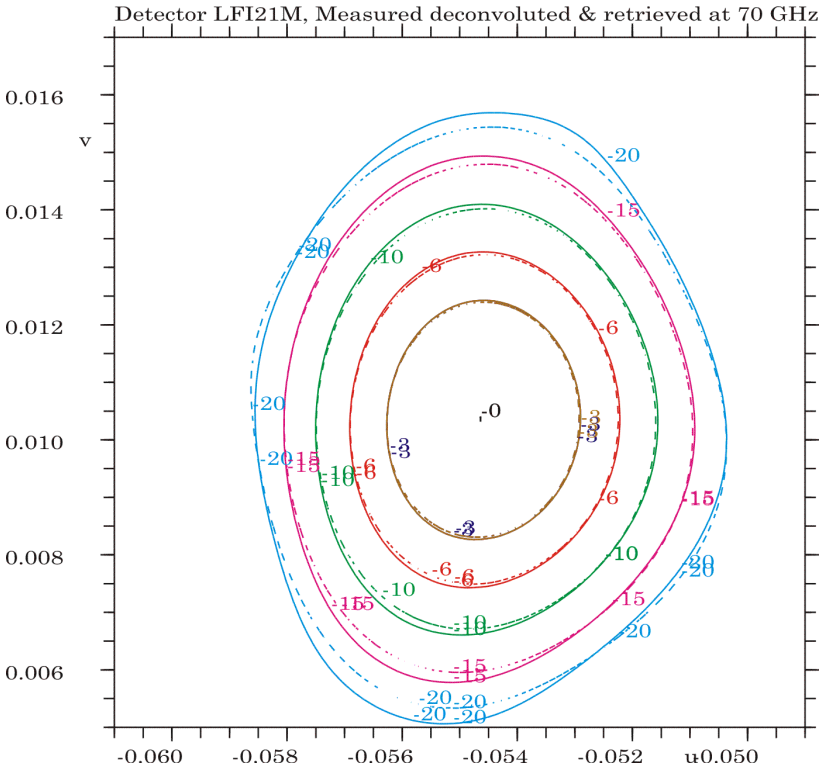

a) Measured (full line) and retrieved (dashed) power pattern

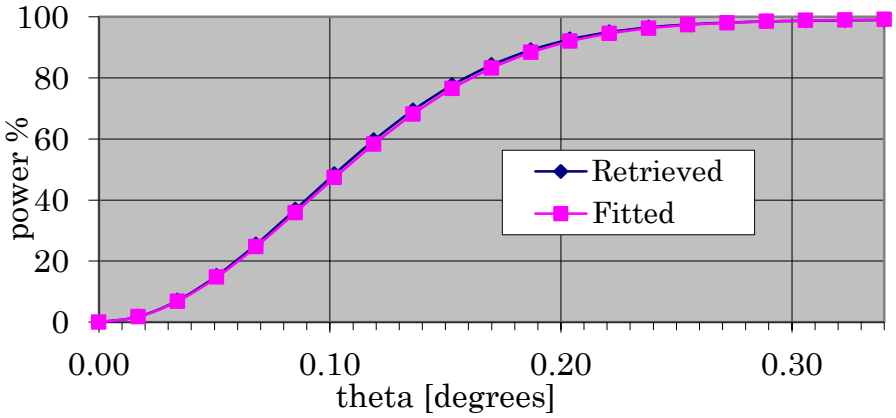

b) Azimuthally integrated power

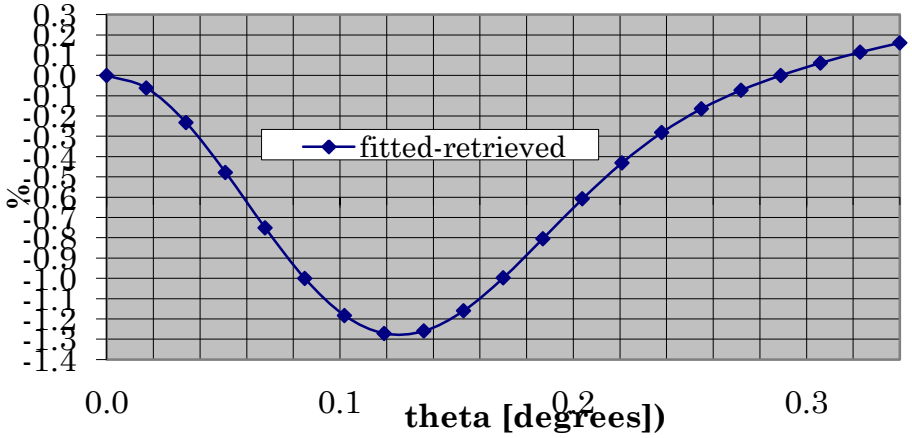

c) Difference

Figure 2-18 Kriging fitted measured and retrieved power pattern for 70 GHz detector, LFI21M.

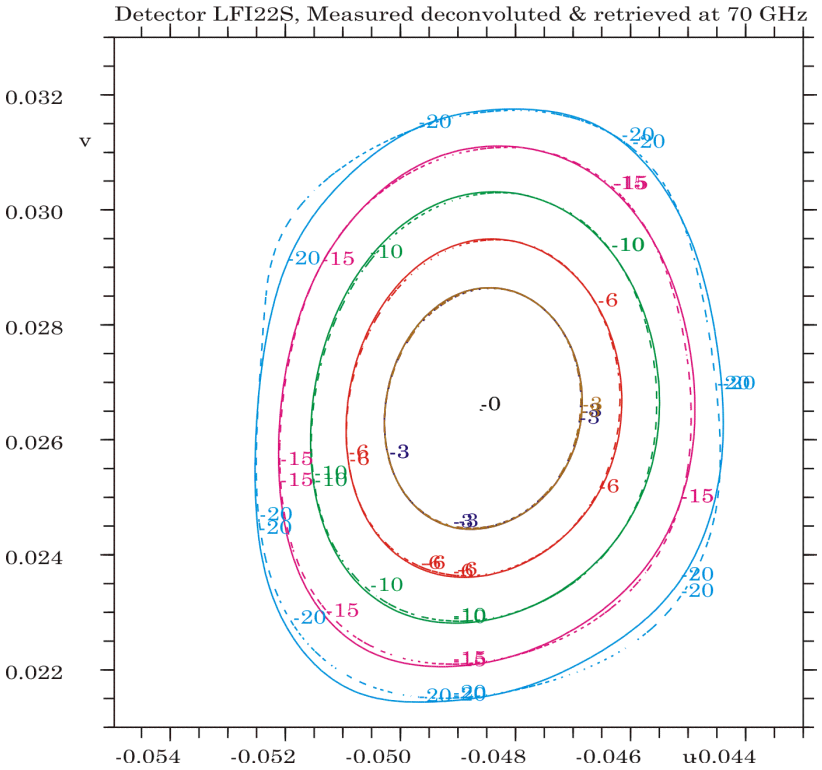

a) Measured (full line) and retrieved (dashed) power pattern

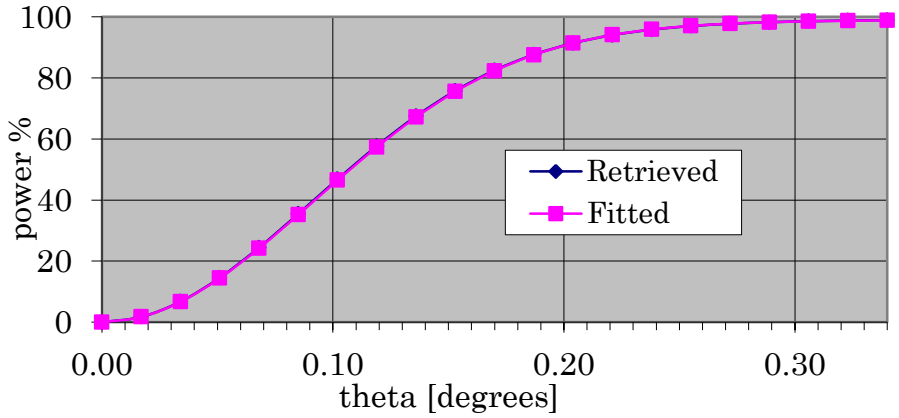

b) Azimuthally integrated power

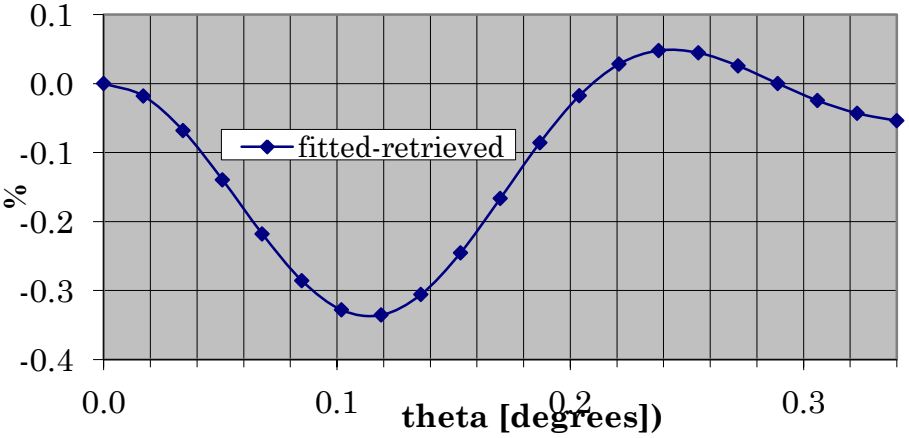

c) Difference

Figure 2-19 Kriging fitted measured and retrieved power pattern for 70 GHz detector, LFI22S.

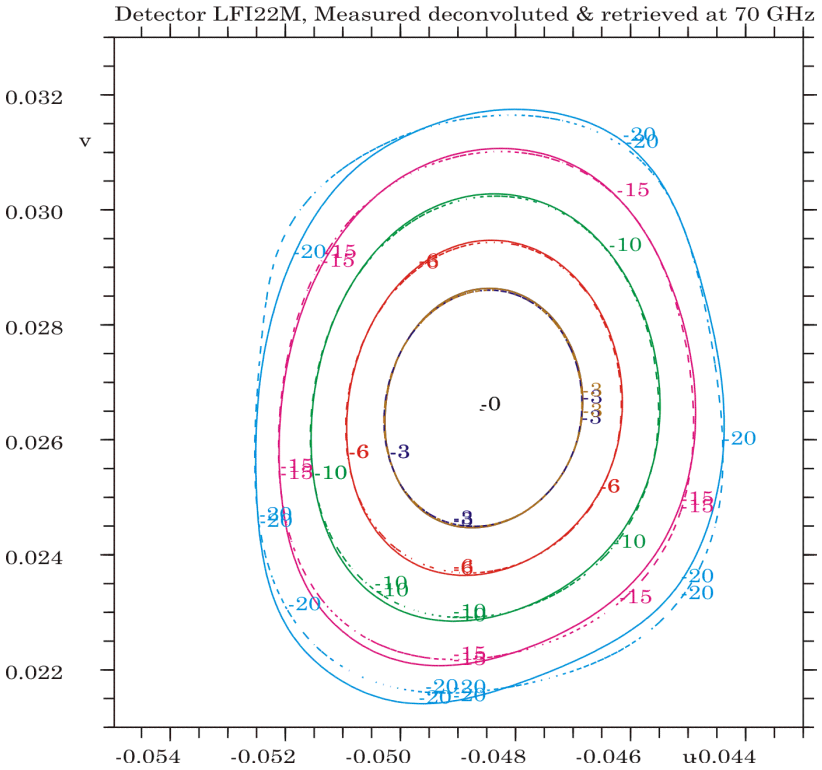

a) Measured (full line) and retrieved (dashed) power pattern

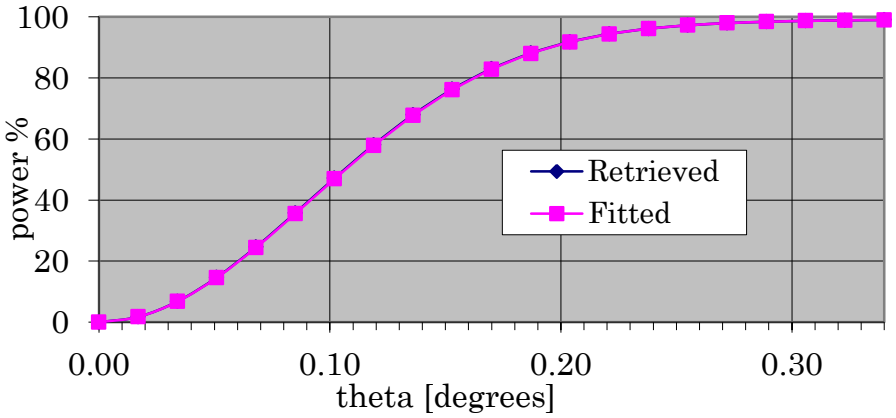

b) Azimuthally integrated power

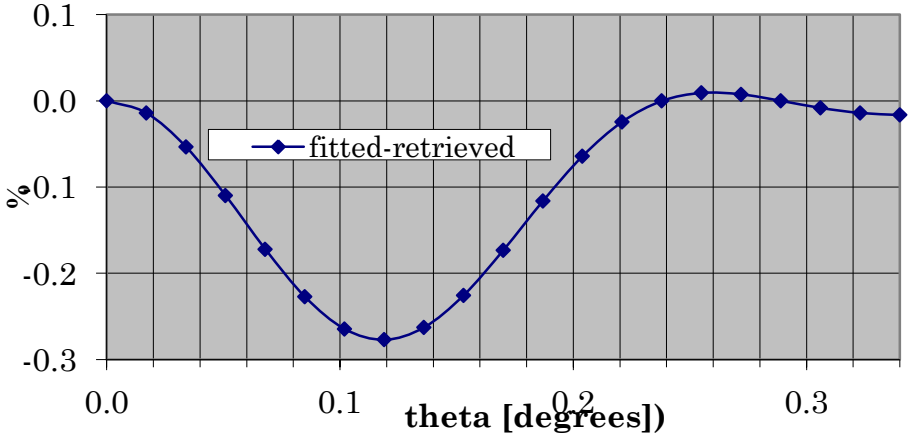

c) Difference

Figure 2-20 Kriging fitted measured and retrieved power pattern for 70 GHz detector, LFI22M.

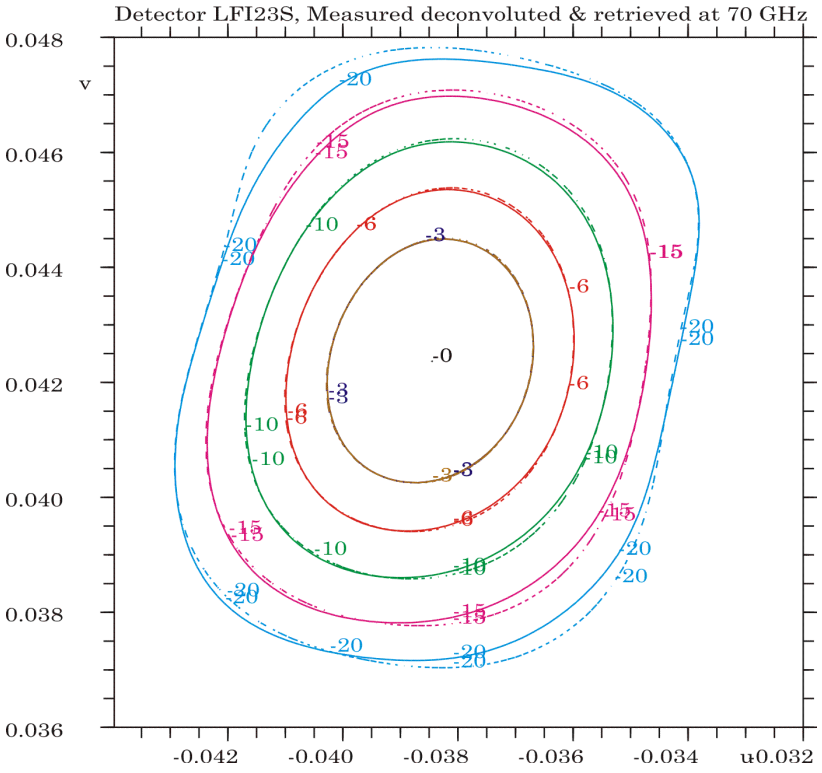

a) Measured (full line) and retrieved (dashed) power pattern

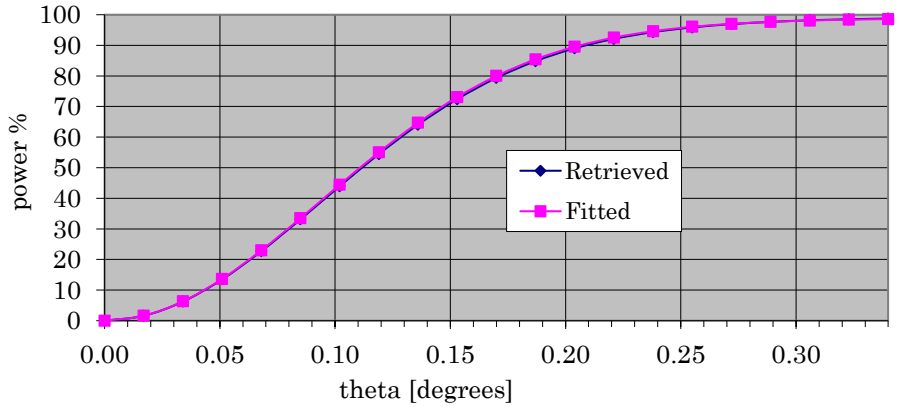

b) Azimuthally integrated power

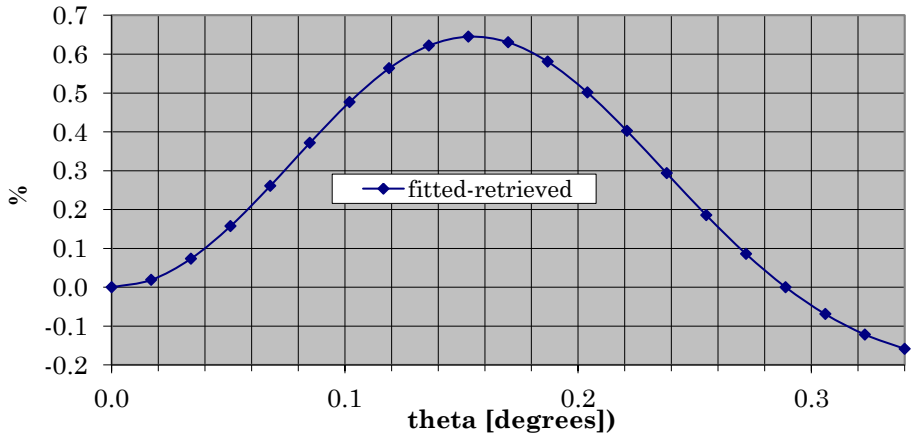

c) Difference

Figure 2-21 Kriging fitted measured and retrieved power pattern for 70 GHz detector, LFI23S.

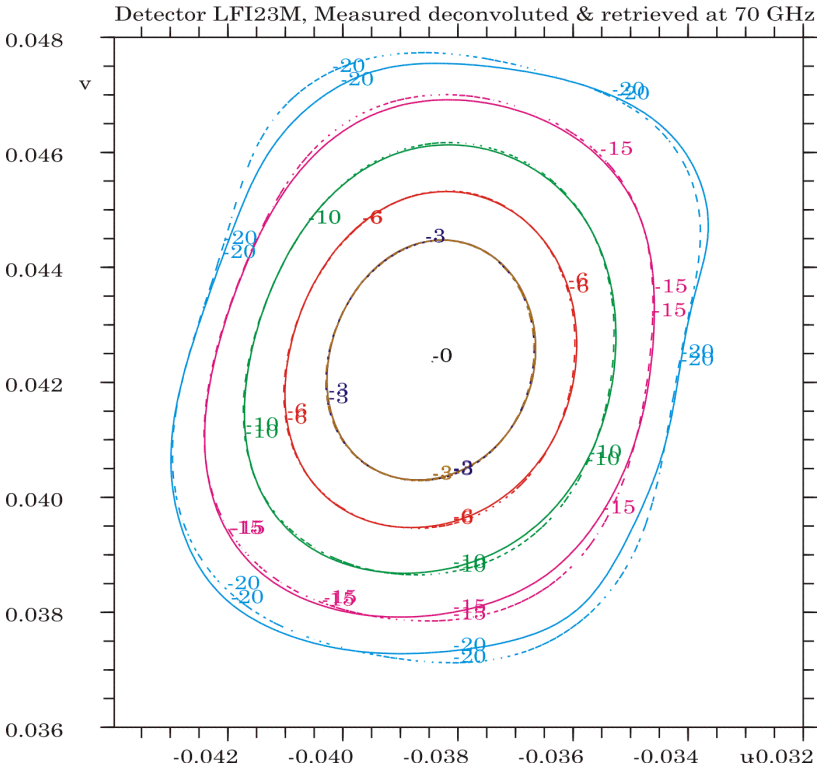

a) Measured (full line) and retrieved (dashed) power pattern

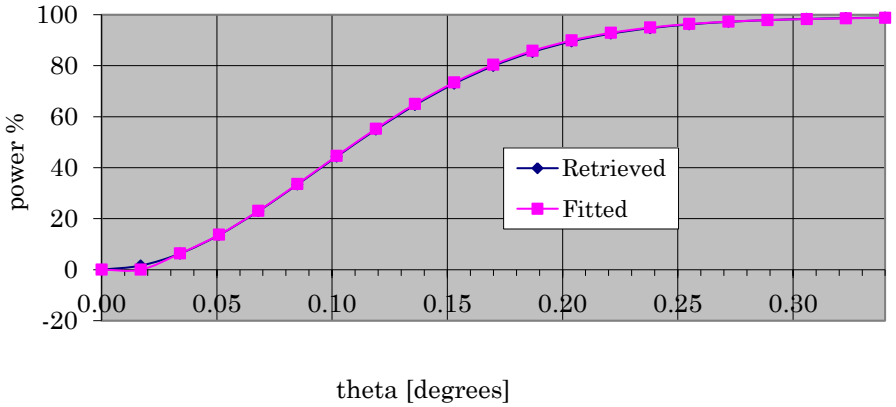

b) Azimuthally integrated power

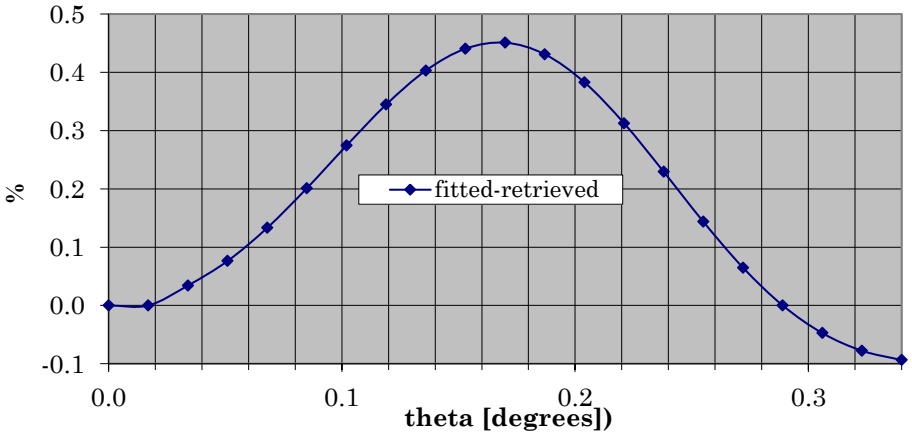

c) Difference

Figure 2-22 Kriging fitted measured and retrieved power pattern for 70 GHz detector, LFI23M.

3. Conclusion.

The RF performances from the final retrieved telescope geometry, RFM2, are shown to be significantly improved upon the RF calculations from the RFFM telescope geometry. The RFFM results are given in Report S-1563-03. The remaining differences between the retrieved and the measured beams are listed in Table 3-1.

LFI		Variance δ [dB]		Max power difference [%]	
Detector	Frequency	S-pol	M-pol	S-pol	M-pol
LFI18	70 GHz	0.08	0.08	0.1	0.2
LFI19	70 GHz	0.10	0.15	0.5	1.0
LFI20	70 GHz	0.15	0.16	1.1	1.3
LFI21	70 GHz	0.17	0.15	1.3	1.1
LFI22	70 GHz	0.08	0.10	0.3	0.3
LFI23	70 GHz	0.10	0.10	0.6	0.5
LFI24	44 GHz	0.10	0.07	0.7	0.1
LFI25	44 GHz	0.13	0.17	0.5	0.5
LFI26	44 GHz	0.10	0.19	0.2	0.2
LFI27	30 GHz	0.13	0.10	0.4	0.3
LFI28	30 GHz	0.14	0.12	0.4	0.3
Total		0.13 dB			

Table 3-1 Remaining LFI variances of RFM2.

The integrated power differences are largest for the 70 GHz beams. The outmost beams are well retrieved, but the other beams are slightly narrower than for the measured patterns. Especially for detector LFI20 and LFI21, where the power difference is up to 1.3%. Compared to the final variances in the retrieval of RFM1, see Report S-1563-09, the 30 GHz beams are improved significantly from 1.2% to 0.3%. This is also the case for LFI18 at 70 GHz with a decrease in power difference from 1.1% to 0.2%.

All the measured and retrieved RFM2 beams are shown together in Figure 3-1 with contour levels down to 20 dB below peak.

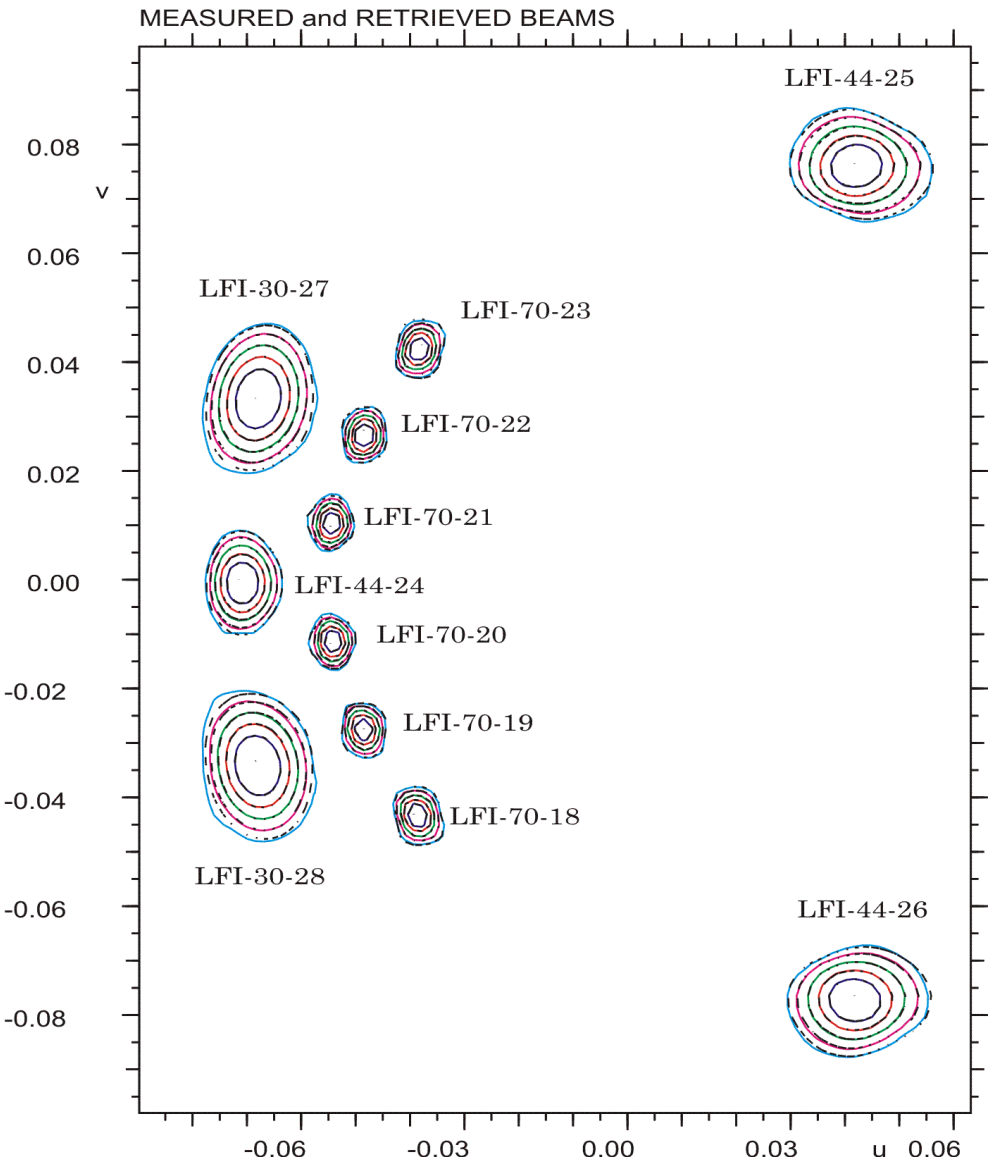

Figure 3-1 All measured and retrieved LFI beams.

References

P. Nielsen, 2013
"In-flight Retrieval of Geometrical information on the Planck Telescope – LFI beam data from Jupiter scan1", S-1563-03, dated April 2013.

P. Nielsen, 2014
"In-flight Retrieval of Geometrical information on the Planck Telescope – Geometry retrieval using LFI beam data from all Jupiter scans", S-1563-09, dated September 2014.

P. Nielsen, 2015
"In-flight Retrieval of Geometrical information on the Planck Telescope – Geometry retrieval using combined HFI and LFI beam data", S-1563-13, dated December 2015.

A. Final RFM2 retrieved geometry

The final retrieved telescope geometry model, RFM2, is described by the following displacements and distortions defined in the telescope coordinate systems shown in Figure A-1.

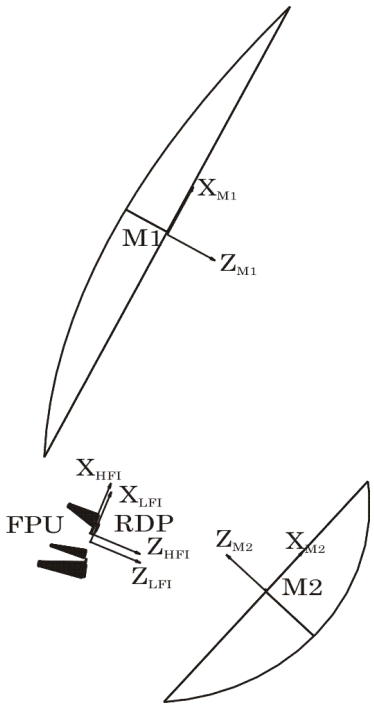

Figure A-1 Coordinate systems for RFM2.

The common LFI FPU coordinate system displacements are

- translation in X_{RDP}-direction of ÷0.06 mm
- translation in Y_{RDP}-direction of ÷0.01 mm
- translation in Z_{RDP}-direction of +0.05 mm
- rotation around the Z_{RDP}-axis of ÷4.1 arcmin

The common HFI FPU coordinate system displacements are

- translation in X_{RDP}-direction of +0.27 mm
- translation in Y_{RDP}-direction of ÷0.11 mm
- translation in Z_{RDP}-direction of +0.26 mm
- rotation around the Z_{RDP}-axis of +0.9 arcmin

All coordinate system displacements and rotations are relative to the respective NRFFM systems with the new detector positions described in Report S-1563-09.

The retrieved surface distortions on the reflectors are defined in the Z_{M1}- and Z_{M2}-directions and represented by the Zernike modes in Table A-1 and Table A-2.

Zernike mode		Amplitude	Rotation
m	n	[mm]	[degrees]
0	0	0.	0
0	2	-0.08	0
1	1	0.99	68
2	2	0.13	79
1	3	0.09	6
3	3	0.06	-58

Table A-1 Retrieved Zernike modes on main reflector.

Zernike mode		Amplitude	Rotation
m	n	[mm]	[degrees]
0	0	0.	0
0	2	0.00	0
1	1	1.37	-35
2	2	0.05	-69
1	3	0.29	-7
3	3	0.03	4

Table A-2 Retrieved Zernike modes on subreflector.

The LFI and HFI feed displacements in the individual retrieved FPU coordinate systems are given in Table A-3 and Table A-4, respectively.

Feed displacements	Deviation from retrieved RDP	
Detector	Δx [mm]	Δy [mm]
LFI18	0.03	0.11
LFI19	0.08	-0.13
LFI20	0.16	0.34
LFI21	-0.43	-0.36
LFI22	0.06	0.08
LFI23	0.15	0.00
LFI24	-0.20	-0.16
LFI25	-0.10	-0.05
LFI26	0.03	0.03
LFI27	-0.14	0.10
LFI28	-0.04	0.09

Table A-3 Retrieved LFI feed displacements.

Displacements	Deviation from RDP	
Detector	Δx [mm]	Δy [mm]
HFI-100-1	-0.05	0.00
HFI-100-2	-0.05	0.08
HFI-100-3	-0.02	0.09
HFI-100-4	**-0.12**	0.09
HFI-143-1	0.01	-0.01
HFI-143-2	0.02	-0.09
HFI-143-3	0.01	-0.08
HFI-143-4	0.01	-0.08
HFI-143-5	0.00	-0.05
HFI-143-6	-0.02	-0.11
HFI-143-7	-0.04	**-0.12**
HFI-217-1	0.04	0.04
HFI-217-2	0.05	0.09
HFI-217-3	0.05	0.14
HFI-217-4	-0.04	0.23
HFI-217-5	0.08	0.07
HFI-217-6	0.03	0.00
HFI-217-7	0.00	0.11
HFI-217-8	0.06	**0.11**
HFI-353-1	0.09	0.02
HFI-353-2	0.07	-0.07
HFI-353-3	0.09	0.03
HFI-353-4	0.10	0.01
HFI-353-5	**0.11**	0.06
HFI-353-6	0.09	0.05
HFI-353-7	0.06	0.01
HFI-353-8	-0.03	-0.01
Average	0.02	0.02

Table A-4 Retrieved HFI feed displacements.